

Direct and Indirect Hydrogen Storage: Dynamics and Interactions in the Transition to a Renewable Energy Based System for Europe

Zhiyuan Xie^{a,*}, Gorm Bruun Andresen^{a,b}

^a*Department of Mechanical and Production Engineering, Aarhus University, Aarhus, Denmark*
^b*iCLIMATE Interdisciplinary Centre for Climate Change, Aarhus University, Aarhus, Denmark*

Abstract

To move towards a low-carbon society by 2050, understanding the intricate dynamics of energy systems is critical. Our study examines these interactions through the lens of hydrogen storage, dividing it into ‘direct’ and ‘indirect’ hydrogen storage. Direct hydrogen storage involves electrolysis-produced hydrogen being stored before use, while indirect storage first transforms hydrogen into gas via the Sabatier process for later energy distribution. Firstly, We utilize the PyPSA-Eur-Sec-30-path model to capture the interactions within the energy system. The model is an hour-level, one node per country system that encompasses a range of energy transformation technologies, outlining a pathway for Europe to reduce carbon emissions by 95% by 2050 compared to 1990, with updates every 5 years. Subsequently, we employ both quantitative and qualitative approaches to thoroughly analysis these complex relationships. Our research indicates that during the European green transition, cross-country flow of electricity will play an important role in Europe’s rapid decarbonization stage before the large-scale introduction of energy storage. Under the paper cost assumptions, fuel cells are not considered a viable option. This research further identify the significant impact of natural resource variability on the local energy mix, highlighting indirect hydrogen storage as a common solution due to the better economic performance and actively fluctuation pattern. Specifically, indirect hydrogen storage will contribute at least 60% of hydrogen storage benefits, reaching 100% in Italy. Moreover, its fluctuation pattern will change with the local energy structure, which is distinct difference with the unchanged pattern of direct hydrogen storage and battery storage.

Keywords: Interactions, PyPSA-Eur-Sec-30-path, Hydrogen Storage, Volatility Analysis

1. Introduction

The global energy landscape is undergoing significant challenges due to escalating demands from a booming population [1]. As evidence of climate change’s adverse impacts accumulates, the urgency of transitioning to greener energy sources becomes urgent [2]. The discourse on this green transition often emphasizes the integration of energy systems, which can enhance energy efficiency and mitigate decarbonization expenses [3, 4]. For instance, the incorporation of wind-solar hybrid systems enhances both diurnal and seasonal energy accessibility, minimizing the need for extensive energy storage investments [5, 6]. Similarly, combined heat and power systems amplify the overall efficiency of the energy system [7, 8]. Nevertheless, the integration of diverse renewable technologies introduces complex interactions within the energy system. In this paper, we seek to improve the comprehension of intricate dynamics in these new complex energy systems, specifically through the lens of hydrogen in its direct and indirect storage forms. Our goal is to use this understanding to guide and facilitate the green transition in a broad sense.

At this juncture, it’s essential to review current literature to grasp how different studies perceive the interplay within the en-

ergy system, especially among renewable energy, storage, and electricity transmission. The electricity sector is witnessing transformative changes with the integration of renewable energy sources (RES), especially wind and solar [9, 10]. Historically, fossil fuel costs were the primary determinants of electricity prices. However, as RES adoption grows, this paradigm is shifting [11, 12]. One of the notable challenges introduced by these renewables is their intermittency, which impacts electricity pricing [13, 14]. In situations where wind and solar outputs peak, the marginal cost of electricity generation drastically decreases. This has led to moments of ultra-low, and sometimes even negative, electricity prices [15, 16]. De Vos [16] suggests that the shift towards renewables reduces dependence on fossil fuels, potentially lowering electricity prices, especially in competitive market regions. Implementing CO₂ allowance prices emerges as a solution to counter negative market prices. Furthermore, the inability to store large amounts of electricity aggravates pricing challenges. Such limitations induce price volatility, underscoring the intricate dance of balancing electricity supply with demand [17].

To facilitate and advance the large-scale integration of renewable energy into the energy system, energy storage is increasingly seen as an indispensable solution, emerging as a central pillar of the contemporary energy framework [18, 19]. Currently, pumped hydropower storage dominates the global energy storage landscape. However, its potential is somewhat re-

*Corresponding author.

Email address: zyx@mppe.au.dk (Zhiyuan Xie)

stricted due to terrain prerequisites, a limitation particularly evident in Europe where most of its potential has been tapped [20]. Batteries often serve as the preferred choice for short-duration energy storage, whereas hydrogen (H_2) is seen as a promising long-duration storage alternative [21, 22]. Areas that face pronounced electricity price fluctuations, owing to the variability of renewable energy sources, typically witness a spike in investments geared towards storage infrastructure [23]. However, the role of energy storage in green transitions isn't universal; its significance can differ based on various sector coupling scenarios, as meticulously explored by Victoria *et al* [24]. This evolving landscape underscores the intertwined nature of renewable energy generation, electricity pricing, and energy storage.

Cross-country flow of electricity is a pivotal factor differentiating various energy scenarios. While many existing research models overlook the intricacies of interconnections between countries or regions [25], the benefits of such interconnections are undeniable. Enhancing cross-country electricity flow and sector coupling simultaneously can create synergies that yield significant benefits [26]. Enhanced power transmission not only alleviates grid congestion but also ensures the smooth integration of renewable energy, subsequently influencing electricity prices. Moreover, robust interconnections pave the way for more streamlined electricity markets, fostering competitive pricing. Such pricing structures not only benefit consumers but also guarantee consistent electricity supplies [27, 28, 29]. Even in scenarios where bolstering transmission is viewed with skepticism, either due to perceived challenges or economic concerns [30], the significance of current transmission capabilities and the potential for expansion should not be sidelined.

Current research extensively explores the interplay between different components of the energy system, while often under lots of restrictive assumptions. This focus predominantly on local connections between a few energy sectors results in a narrow view, largely overlooking the broader, interconnected dynamics of the energy landscape [25]. Such a limited perspective tends to underestimate the potential of some renewable energy technology by not fully accounting for its capabilities and impact when integrated on a larger scale. Consequently, there's a pressing need for studies that transcend these local confines to offer a more holistic understanding of the energy system. To address these limitations and provide a more encompassing view of the energy transition, this paper will utilize the PyPSA-Eur-Sec-30-path model developed by Victoria *et al* [31]. This model offers valuable insights into the overall energy transition process by presenting a scenario of transitioning to high renewable energy reliance within the context of interconnectedness across 30 European countries. It encompasses a range of necessary renewable energy-related technologies and delves into the impacts of different CO_2 emission reduction trajectories on green transition costs. Their research concludes that initiating emission reductions early and maintaining a steady pace is more cost-effective than delayed, rapid reductions. Building on this finding, this paper focuses on the nuanced interactions observed under the strategy of early and consistent emission reduction.

Based on having a comprehensive vision for the transformation of the energy system, this paper utilizes hydrogen storage

as a key entry point to unravel the complex interactions within the system, due to its significant intersections with the heating, power, and gas sectors. In line with this vision, this paper introduces innovative concepts of 'direct' and 'indirect' H_2 storage, pivotal in understanding H_2 's integral function across these diverse sectors. This conceptual framework enables the study to expand further, exploring a range of technologies within the energy model and highlighting the multifaceted nature of energy transitions. To analyze the dynamics of various renewable technologies comprehensively, this research employs a combination of Fast Fourier Transform (FFT), Continuous Wavelet Transform (CWT), and Cycle Capture (CC) methods. These approach deepens our understanding of the time-dependent behavior and interactions of different elements in the energy system.

The structure of this paper is as follows: Section 2 provides a concise introduction to the research model and methods employed and elucidates the concepts of direct and indirect hydrogen storage. A detailed mathematical description of the model is available in the Appendix A for further reference. Section 3 ventures into an exploration of the intricate interdependencies within the energy system, offering insights from various analytical angles. While section 3 includes select illustrative figures, a full set of corresponding diagrams is housed in Appendix B for completeness. Finally, Section 4 summarizes the key findings and conclusions drawn from this study.

2. Methods

2.1. Model Description and Hydrogen Storage

The PyPSA-Eur-Sec-30-path model [31] stands as an open-source network model of the European energy system, featuring hourly resolution and a single-node representation for each country. In this paper, the scope of the model includes the electricity, heating, hydrogen and gas sectors. The full network consists of 30 nodes, representing the 28 EU member states as of 2018, excluding the islands of Malta and Cyprus. However, it extends to include the well-connected non-EU countries Norway, Switzerland, Serbia, and Bosnia-Herzegovina. Each of these neighboring countries is interconnected through high voltage transmission lines.

The PyPSA-Eur-Sec-30-path model employ a brownfield optimization approach, which includes existing power plant capacities until the end of their technical lifetime. In addition to these, the model may invest in new energy infrastructure to cover the energy demands. To analyze a decarbonization pathway for the European power system, a myopic approach is used. This approach, characterized by limited foresight over the investment period [32]. This approach may incur higher overall system costs compared to perfect foresight optimization due to stranded investments.

Figure 1 represent a schematic of a multi-vector energy system, integrating various sources and forms of energy into a cohesive network. That is, the schematic diagram of PyPSA-Eur-Sec-30-path model. The system is organized into four primary

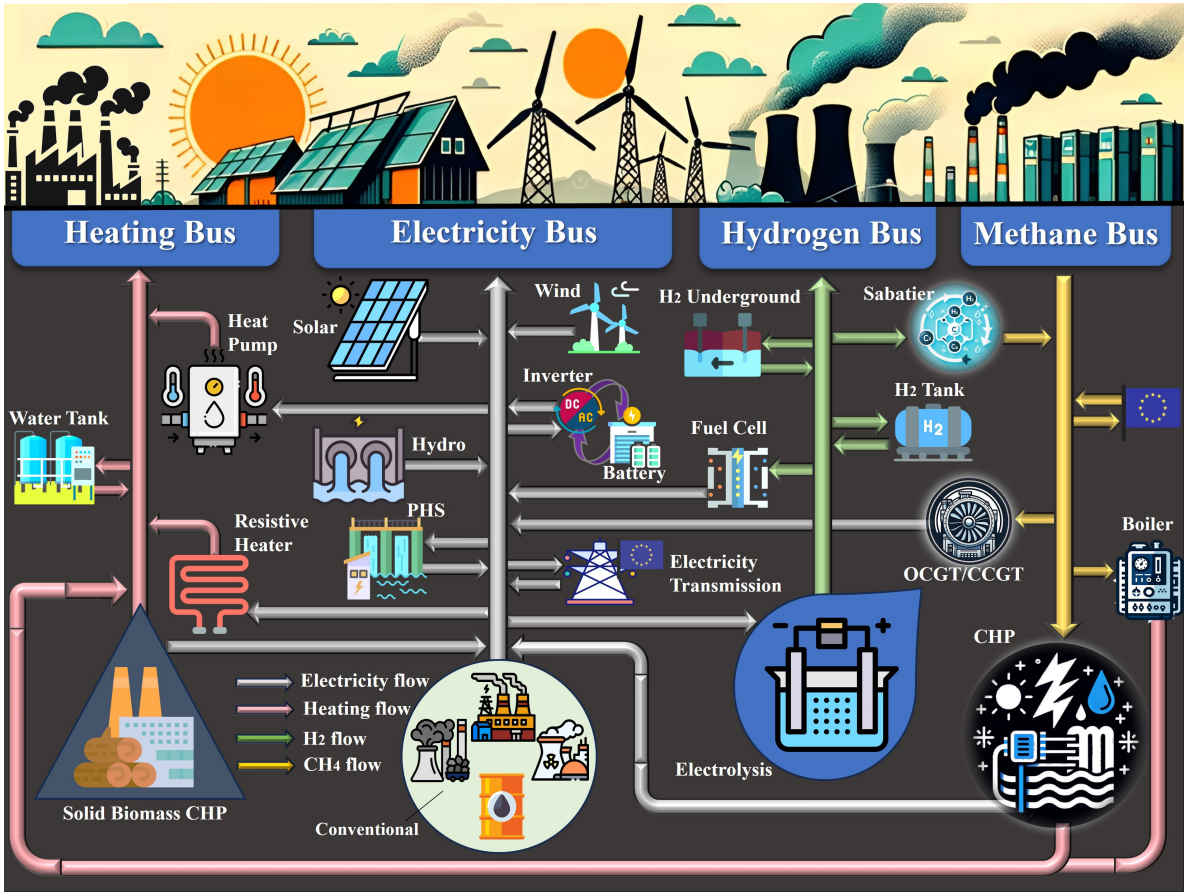


Figure 1. Energy Flow Dynamics in Country-Specific Nodes: An Analysis of Electricity, Heating, Hydrogen, and Methane Buses with Technological Correlations. (Icons sourced from Flaticon.com and OpenAI, available for free use).

'buses', each corresponding to distinct energy carriers: Heating, Electricity, Hydrogen, and Methane, illustrating various technologies and processes within.

Central to the system, the Electricity Bus interfaces with renewable sources, including solar, wind, and hydroelectric stations, alongside solid biomass. It also encompasses conventional power plants powered by oil, lignite, coal, or nuclear energy, highlighting the synergy between traditional and renewable energy sources. The inclusion of storage solutions—such as a combination of inverters and batteries, pumped-hydro storage (PHS), and hydrogen storage - underscores their importance in a renewable-dominant energy landscape. The Electricity Bus serves as a nexus, supplying or receiving energy from other buses and nations. It interconnects with the Methane Bus via Sabatier technology, cycling methane back through various power generation technologies. Additionally, it distributes electricity to heating applications and connects with other national grids through high-voltage direct current (HVDC) systems. Notably, the conventional power plants, hydroelectric stations, and PHS are exogenously fixed in the model. All except hydroelectric stations, and PHS are subject to decommissioning upon reaching their technical lifespan.

The Heating Bus includes two different configurations, depending on population density: one for urban heating and another for rural heating. In urban areas with high popula-

tion density, a variety of technologies are integrated into district heating networks to supply heating. These include central ground-sourced heat pumps, heat resistors, gas boilers, and combined heat and power (CHP) units. Additionally, individual air-sourced heat pumps are available as an option in these urban settings. Conversely, in rural, low-density population areas, heating is typically provided by individual installations, such as ground-sourced heat pumps, heat resistors, and gas boilers, catering to the specific needs of these less populated regions.

The Hydrogen Bus is characterized by electrolysis units that produce green hydrogen using electricity, presumably from renewable sources in the late Europe green transition stage. While underground storage represents a large-scale solution, geological constraints necessitate the inclusion of above-ground H₂ storage tanks within the model. The hydrogen flow is dynamic, serving either storage or immediate conversion to methane via the Sabatier process. Hydrogen may also be provided to fuel cells for direct conversion to electricity.

Lastly, the Methane Bus features the Sabatier process for synthesizing natural gas from hydrogen and carbon dioxide, with CHP units indicating methane's role in both heating and power generation. Boilers for heating and turbines for electricity production further highlight the dual utility of methane in this integrated system. This illustrates that methane, derived from the Hydrogen Bus, serves a dual purpose: it meets de-

mands for both heating and electricity. And we can conclude hydrogen may operate in our model through 5 distinct pathways, which are:

- 1) **Electrolysis - Store - Fuel Cell (ESFC):** Hydrogen is produced, stored, and then used in fuel cells to generate electricity that meets power demands on the electricity bus.
- 2) **Electrolysis - Store - Sabatier - Electricity (ESSE):** Hydrogen is produced, stored, and then used in the Sabatier reaction to create gas that powers Combined Heat and Power (CHP) units, Open-Cycle Gas Turbines (OCGT), or Combined-Cycle Gas Turbines (CCGT), generating electricity to fulfill electricity bus requirements.
- 3) **Electrolysis - Store - Sabatier - Heating (ESSH):** Hydrogen is produced, stored, and then used in the Sabatier reaction to produce gas for CHP systems or boilers, providing heat to satisfy heating demands.
- 4) **Electrolysis - Sabatier - Store - Electricity (ESE):** Hydrogen produced through electrolysis is utilized in the Sabatier reaction to synthesize gas. This gas is then stored and subsequently dispatched as needed for electricity generation through CHP, OCGT, and CCGT, which in turn supply the electricity bus.
- 5) **Electrolysis - Sabatier - Store - Heating (ESH):** Following electrolysis, hydrogen is immediately processed via the Sabatier reaction to produce gas. This gas can either be stored directly in gas storage or immediately used in CHP and boilers. The energy generated by these systems can then be stored as heat in thermal storage units. Finally, the heating energy will provide to the heating bus.

And here is no doubt that the pathway 1 to 3 belongs to the H₂ storage, and we called it ‘direct’ H₂ storage. However, the pathway 4 and 5 both involves the electrolysis, which can also be considered a form of storage since it utilizes surplus electricity from the electricity bus to store energy in another form [33]. Therefore, we categorize the pathway 4 and 5 as ‘indirect’ H₂ storage, highlighting their role in energy conversion and storage.

Overall, the schematic illustrates a complex, integrated energy system that leverages multiple energy carriers and storage solutions to maximize efficiency and utilize renewable energy sources. For an in-depth exploration of the model and technologies involved, such as the COP of heat pump, land use constraints and the detail of the solid biomass, the reader is directed to Victoria *et al.* [31].

2.2. Basis for Country Case Selection

Diverse geographical landscapes and natural resource endowments across Europe lead to varying renewable energy potentials among different countries. As Figure 2 illustrates, by 2050, Denmark (DNK) is expected to harness predominantly wind energy, Germany (DEU) to utilize a balanced mix of wind and solar, and Italy (ITA) to rely heavily on solar power. This

projection underscores the distinct energy generation methods that each country will likely adopt. Such differences are crucial for this paper, it means the energy transition path in Denmark, Germany, and Italy emerges as typical or extreme subjects to represent the spectrum of energy transition outcomes from 2020 to 2050. Moreover, A comparative analysis of these distinct countries will specifically account for the influence of natural resource variability on the energy transition, thereby enriching our understanding with a more holistic perspective.

Due to space constraints, the Results and Discussion section of this paper will primarily focus on graphical relevant to Germany. Comprehensive graphical for Denmark and Italy, while not featured in the main section, are included in the Appendix B for thorough examination. The analysis in this section will commence with the findings pertinent to Germany, followed by detailed examinations of Denmark and Italy, ensuring a comprehensive discussion across all three countries.

2.3. Mathematical Modelling

For a detailed explanation of the mathematical foundation of the PyPSA-Eur-Sec-30-path model, please refer to Appendix A. This appendix details the model’s minimum cost objective function, the equilibrium constraints for supply and demand, and the pathway for CO₂ emissions reduction.

It is essential to emphasize that the electricity prices at specific nodes (with one node representing each country) are derived from the power supply and demand balance constraints at those respective nodes, meaning the electricity price used in this study are locational marginal prices (LMP). The same pricing principle applies to hydrogen. Similarly for the hydrogen price. From an economic perspective, this marginal price indicates the additional cost incurred for delivering one more unit of electricity or hydrogen to a particular node. It’s crucial to recognize that this price is not a standalone number, it is the result of the dynamic interactions between multiple elements of the energy system.

In the Mathematical Modelling section, the primary focus will be on the mathematical formulation of the economic indicators and the qualitative analysis methods employed.

2.3.1. Mathematical Formulations for Economic Metrics

For the economic indicators, we mainly examine the Levelized Cost of Storage (LCOS), Unit Benefit (UB), overall price spread (OPS) and Cycle Frequency (CF). The Levelized Cost of Storage (LCOS) mathematical expressions are as follows [34]:

$$LCOS = \frac{\sum_{t=0}^T C_{\text{total cost},t}}{\sum_{t=0}^T E_{\text{dis},t}} \quad (1)$$

The term $\sum_{t=0}^T C_{\text{total cost},t}$ represents the accumulated annualized cost, which includes consideration of the discount rate at 7%. For storage, the total cost typically encompasses the accumulated annualized cost in parts of the charging link (such as electrolyzers or battery inverters), the storage system itself, and the discharging link (such as fuel cells). However, for H₂ work pathways 4 and 5, since the H₂ is transported directly from electrolysis to the Sabatier process, the accumulated annualized

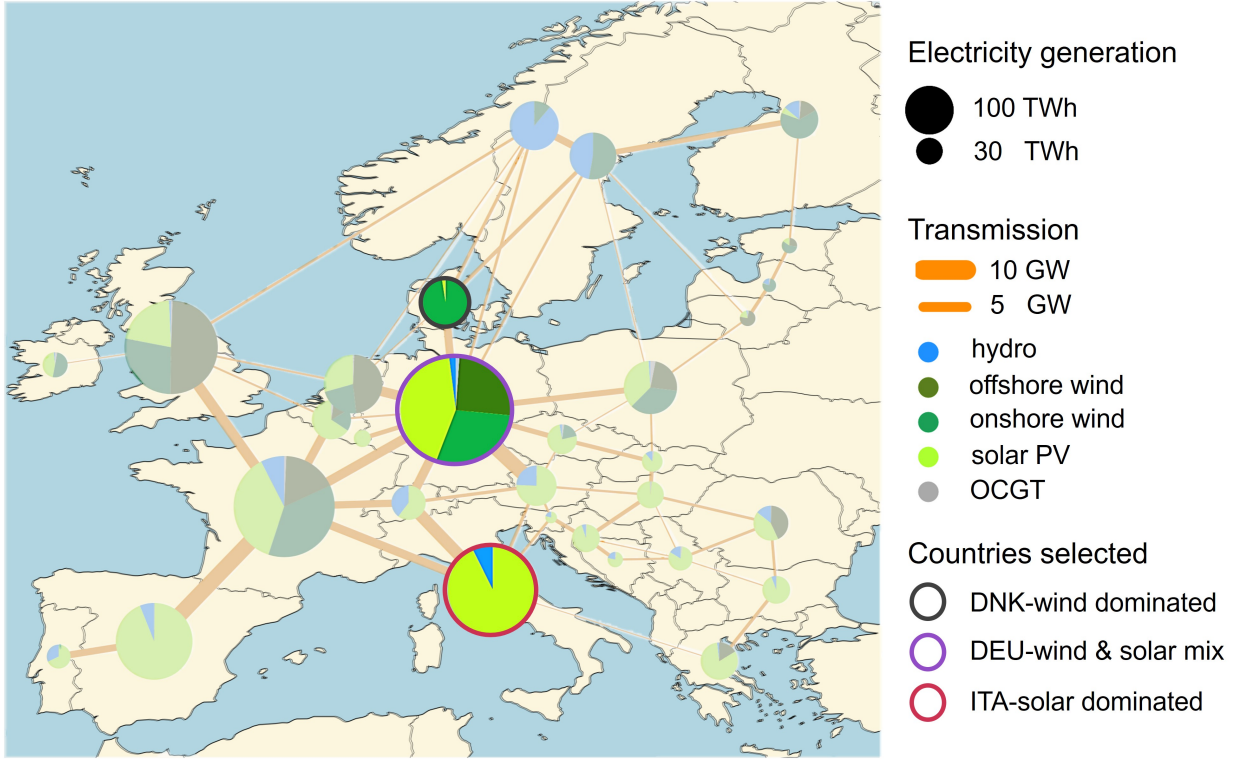


Figure 2. Diverse Energy Mixes in European Electricity Generation by 2050 (Denmark, Germany, Italy Highlighted), adapted from Victoria *et al.* [31], Figure 6.

cost for the storage itself is not included in the calculation of the total cost. It is important to note that $\sum_{t=0}^T E_{\text{dis},t}$ refers to the amount of energy available for discharge, calculated prior to considering discharge efficiency. This approach facilitates a straightforward comparison across different H₂ work pathways and battery systems by placing them on a uniform benchmark.

The Unit Benefits (UB) mathematical expressions are as follows:

$$UB = \frac{\sum_{t=0}^T R_{\text{cost},t} - \sum_{t=0}^T C_{\text{charging cost},t}}{\sum_{t=0}^T E_{\text{dis},t}} \quad (2)$$

In this context, $\sum_{t=0}^T R_{\text{cost},t}$ refers to the revenue generated from the sale of H₂ to the Sabatier process or from selling electricity to the electricity grid. $\sum_{t=0}^T C_{\text{charging cost}}$, on the other hand, denotes the cost incurred from purchasing electricity from the electricity bus.

The overall price spread (OPS) mathematical expressions are as follows:

$$OPS = \frac{1}{N} \sum_{c=1}^N (P_{\text{sell},c} - P_{\text{buy},c}) \quad (3)$$

While $P_{\text{sell},c}$ is the selling price per unit of energy during cycle c , $P_{\text{buy},c}$ is the selling price per unit of energy during cycle c , N is the total number of cycles detected by the Cycle Capture (CC) method over a year. For detailed information on the CC method and its mechanism for collecting cycle data, please see Section 2.4.

2.3.2. Mathematical Formulations for Qualitative Analysis Methods

During this stage, we apply a combination of Fast Fourier Transform (FFT), Continuous Wavelet Transform (CWT), and Cycle Capture (CC) methodologies. These techniques are employed to meticulously analyze time series data pertaining to storage capacities, renewable energy generation, electricity pricing, and the marginal price of hydrogen. However, the detailed exposition of the Cycle Capture (CC) method is reserved for Section 2.4.

The Fast Fourier Transform (FFT) and the Continuous Wavelet Transform (CWT) are key mathematical tools for analyzing and interpreting data volatility. FFT decomposes a time-based signal into its constituent frequencies, facilitating the detection of frequency components within time series data. On the other hand, CWT provides a more detailed view of non-stationary signals, with frequency components that change over time [35]. However, it's important to note that CWT may emphasize larger scales (lower frequencies) more, as the wavelets at larger scales cover a broader range in frequency space, thus potentially dominating the energy of the CWT, especially when using a logarithmic scale spacing [36]. While FFT can correctly determine the main frequency of the data, it has resolution limitations in time-frequency representation, and assumes that the frequency components of the signal do not vary over time [35]. Consequently, it cannot provide the exact time and frequency of the signal simultaneously. In this study, we employ FFT to capture the frequency characteristics of time series data, and CWT to reveal the internal frequency variation over time.

The Fast Fourier Transform (FFT) mathematical expressions are as follows:

$$X(k) = \sum_{m=0}^{J-1} x(m) \cdot e^{-\frac{2\pi i}{J} km} \quad (4)$$

Where $X(k)$ is the output of FFT for each value of k , $x(m)$ means the input time series data, J represents the number of samples.

The Continuous Wavelet Transform (CWT) mathematical expressions are as follows [37]:

$$X_w(a, b) = \frac{1}{|a|^{1/2}} \int_{-\infty}^{\infty} x(t) \overline{\psi\left(\frac{t-b}{a}\right)} dt \quad (5)$$

where $\psi(t)$ is a continuous function known as the mother wavelet, and the overline represents the complex conjugate operation. And the mother wavelet used in this paper is the Morlet wavelet. The Morlet wavelet is advantageous for its balance between time and frequency localization, offering a good compromise for analyzing signals with time-varying frequencies [38]. And the mathematical expressions are as follows:

$$\psi(t) = e^{-t^2/2} \cos(5t) \quad (6)$$

2.4. Integration of FFT, CWT, and CC Methods for Advanced Analysis

The combination of CWT and FFT offers numerous benefits, enabling the identification of dominant frequencies within the data and tracking how these frequencies vary over time. However, when the large-scale features in the data are prominent, smaller scale features, such as the diurnal fluctuations (24h) of H_2 , may be diminished, while that of Battery would not be affected.

To address this, we introduce a method similar to rainflow-counting method to capture cycles in the time series data, termed the Cycle Capture (CC) method, complementing FFT and CWT. In the CC method developed by this paper, users have the flexibility to adjust data filtering thresholds, as well as rising (charging) and falling (discharging) thresholds, to effectively capture cycle information. For instance, in our study on tracking cycle information in the variation of the battery storage filling level data over a year, only the processes where charging and discharging exceed 10% of the normalized value are identified together as a cycle. Notably, this method is capable of handling data that initiates in any state—waiting, charging, or discharging—ensuring that no initial state or relevant information is overlooked in cycle detection. For a detailed understanding of the CC method's operational logic, please refer to Figure S1. Additionally, the source code for the CC method can be found in Section 2.6.

CC provides two primary advantages in synergy with FFT and CWT:

- 1) Short-Term Fluctuation Detection: The CC method is adept at capturing minor fluctuations in data, mainly observed on daily to weekly time scales, due to the small threshold used in this study. This ability ensures that

while FFT and CWT identify dominant long-term or large-scale patterns in data, CC pinpoints the smaller, more nuanced fluctuations, providing a comprehensive view of both macro and micro data trends.

- 2) Result Verification: When dominant patterns in the data predominantly consist of short cycles, results from FFT, CWT, and CC might converge, highlighting these frequent short-term fluctuations. Such convergence signifies the robustness of the findings, as short-term results from FFT and CWT can be cross verified with CC. This cross validation not only emphasizes commonalities but also affirms the selected threshold's appropriateness for CC, ensuring that all methods align in their analytical objectives.

In short, the synergistic application of FFT, CWT, and CC offers a comprehensive understanding of the data's true volatility, aiding in the exploration of interactions within various sectors of the energy system. Specifically, FFT identifies the primary frequency of the data, CWT traces frequency variations over time, and CC emphasizes short-term frequency information potentially overlooked by FFT and CWT. Moreover, when the dominant frequency exhibits short-term fluctuations, both FFT and CWT can validate the appropriateness of the parameter settings in CC.

Besides the benefits gained from integrating FFT and CWT, CC method is independently used in this study to investigate the intricate interactions within the energy system. This is because CC effectively tracks the start and end index of each cycle, laying the groundwork for the calculations in Equation 3.

2.5. Key Parameter

2.5.1. Input and Output Data

In this study, the load side demand is determined using a variety of 2015 data sources. Hourly electricity demand for each country is derived from data provided by the EU Network Transmission System Operators of Electricity (ENTSO-E), which is further refined by the Open Power System Data (OPSD) initiative. Additionally, annual heat demand is converted to an hourly resolution using population-weighted temperature time series. For the generation side, country-specific onshore and offshore wind capacity factors are modeled by transforming wind velocity data from the Climate Forecast System Reanalysis (CFSR) into wind generation estimates. Similarly, for photovoltaic (PV) generation, it is assumed that 50% of the PV capacity consists of rooftop installations. Land use considerations involve aggregating suitable land in each reanalysis grid cell based on the Corine Land Cover (CLC) database, while excluding Natura 2000 protected areas. This approach draws on the comprehensive data source overviews provided in studies by Brown *et al.*, Zhu *et al.* [31, 26, 39], Winterscheid *et al.* [40], who emphasize the importance of data quality for result accuracy. The input data used in our model are sourced from open, transparent, and extensively verified datasets. Both the input datasets and the model-generated data are publicly available at the repository: <https://zenodo.org/records/4010644>.

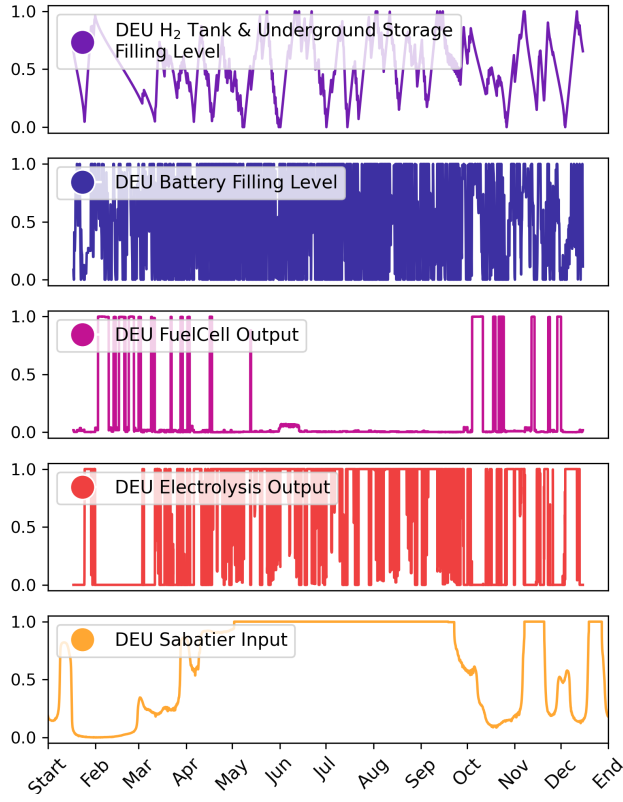


Figure 3. Time Series Analysis of Germany’s Hydrogen Sector and Battery Storage for 2050

Figure 3 offers a detailed visualization of the technological original time series data within Germany’s hydrogen bus, specifically targeting the year 2050. It features an array of critical technologies, including Electrolyzers, Fuel Cells, the Sabatier process, as well as Hydrogen Tank and Underground Storage. This figure not only showcases these technologies but also integrates original time series data related to battery technology. While these datasets are derived from model outputs, they play a role in our research. They form the basis for Fourier Transform (FFT), Continuous Wavelet Transform (CWT), and Cycle Capture (CC) analyses. This integration of technology and data analysis offers a comprehensive understanding of the temporal dynamics, highlighting key trends and variations vital for our study’s insights into the future of hydrogen technology in Germany. To access the original time series data for Denmark and Italy in 2050, please refer to Figure S2 located in Appendix B.

2.5.2. Economic Data

Here we provide techno-economic assumptions for several key components in the energy system. This paper assumes that with technological progress and the expansion of manufacturing scale, the economic costs of renewable energy-related technologies will gradually decrease. The detailed changes are shown in Table 1.

2.5.3. Storage Data

When determining key economic indicators like the Levelized Cost of Storage (LCOS), it’s crucial to consider factors including the efficiency and lifecycle of the pertinent energy storage technology. Table 2 provides a detailed overview of parameters associated with this technology. It should be noted that, owing to terrain constraints, Italy was precluded from constructing underground H₂ storage in the model.

2.6. Code Availability

The PyPSA-Eur-Sec-30-path model is available through the repository <https://zenodo.org/records/4014807#X1> IKRyTS-Uk. Code to capture the cycle information in the time series data is available at <https://github.com/Zion-tunan/Capture-Cycle-in-Time-Series-Data>. Moreover, code to plot the figures shown in this paper is available at <https://github.com/Zion-tunan/Direct-and-Indirect-Hydrogen-Storage-Dynamics-of-InteractionsWithin-Europe-s-Highly-Renewable-Energ>.

3. Results and Discussion

3.1. The Energy System Transition Path in Three Countries

In Figure 4, we present a comprehensive overview of the energy transition landscapes in Germany from 2020 to 2050, and display the energy transition landscapes in Denmark and Italy in Figure S3. The two figures detail the evolution of storage capacity, CO₂ emissions, renewable energy generation & curtailment and cross-country flow of electricity across the three countries, offering a comparative insight into their respective energy transitions. Please note that regarding cross-country flow of electricity, positive values represent energy import from other countries, and negative values represent export.

The first subgraph of Figure 4 carefully examines Germany’s carbon emission reductions alongside changes in energy storage capacity over the years. It reveals that energy storage played a minimal role in Germany’s initial rapid decarbonization phase but became increasingly significant in the later stages of deep decarbonization. Notably, battery involvement in decarbonization emerges around 2035. The capacity of electrolyzers, Sabatier processes, H₂ tanks, and underground storage sees a substantial growth by 2050, indicating large-scale involvement in H₂ storage. Concurrently, the capacities of H₂ tanks and underground storage experience significant growth. However, fuel cell capacity remains negligible, suggesting that direct H₂ storage predominantly occurs through the Sabatier process.

The second subgraph illustrates Germany’s significant increase in wind and solar power generation capacity, crucial for achieving decarbonization goals. Up to 2030, wind power serves as the primary decarbonization driver, increasing by 121% compared to 2025. Post-2035, solar power becomes more important, maintaining a steady average annual growth rate of 58% until 2050. This period sees a concurrent rise in both solar power generation and battery capacity, underlining the growing renewable energy penetration in Germany.

Table 1. Overnight investment cost assumptions per technology and year.

Technology	Unit	2020	2025	2030	2035	2040	2045	2050	source
Onshore wind	€/kWel	1118	1077	1035	1006	977	970	963	[41]
Offshore wind	€/kWel	2128	2031	1934	1871	1808	1792	1777	[41]
Solar PV (utility-scale)	€/kWel	398	326	254	221	188	169	151	[42]
Solar PV (rooftop)	€/kWel	1127	955	784	723	661	600	539	[43]
Battery storage	€/kWh	232	187	142	118	94	84	75	[41]
Battery inverter	€/kWel	270	215	160	130	100	80	60	[41]
H ₂ storage underground	€/kWh	3.0	2.5	2.0	1.8	1.5	1.4	1.2	[41]
H ₂ storage tank	€/kWh	57	50	44	35	27	24	21	[41]
Electrolysis	€/kWel	600	575	550	537	525	512	500	[41]
Fuel cell	€/kWel	1300	1200	1100	1025	950	875	800	[41]

Note: In reference [42] and [43], solar PV investment cost is expressed in 2019-euros. It has been translated into 2015-euros, assuming a growth rate of 2%. For complete parameters, see Supplementary Table 4 in [25].

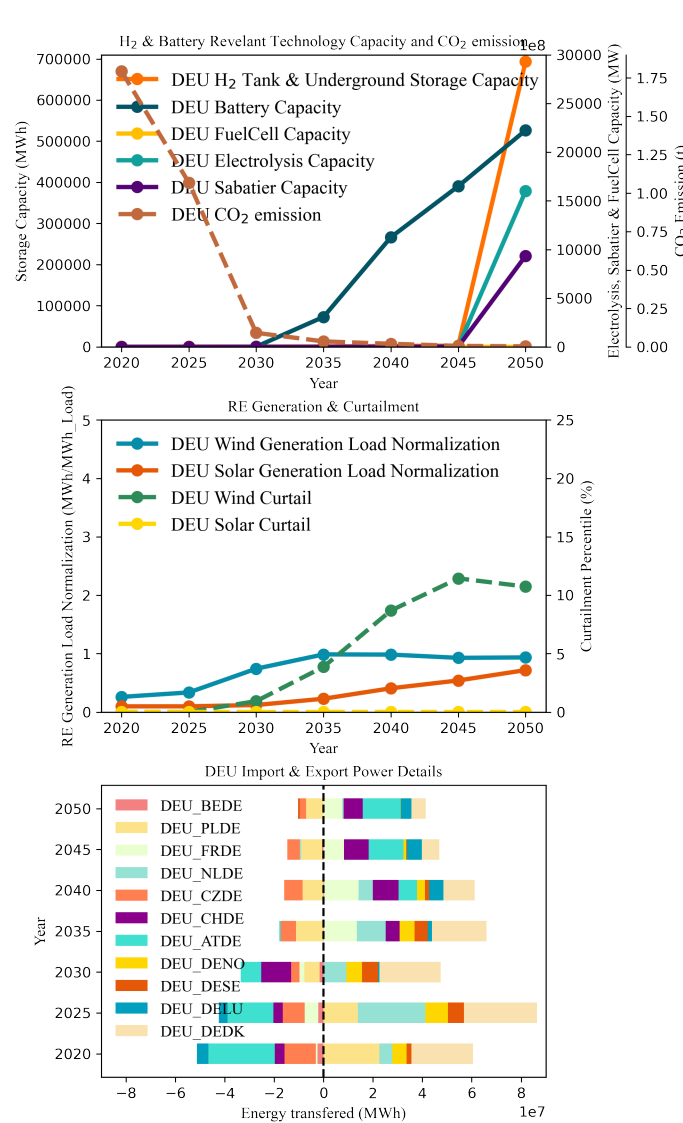


Figure 4. Evolution of Germany's Energy Transition Landscape: Storage Capacity, CO₂ Emission, Renewable Generation & Curtailment, and Cross-country Flow of Electricity (2020-2050)

Table 2. Technical details of storage

Tech	Unit	FOM	Life	Effi.	Source
Battery storage	kWh	0.0	20		[41]
Battery inverter	kWel	0.2	20	0.9	[41]
H ₂ storage underground	kWh	2.0	100	1.0	[41]
H ₂ storage tank	kWh	1.1	25		[41]
Electrolysis	kWel	5.0	25	0.8	[41, 44]
Fuel cell	kWel	5.0	10	0.58	[41, 44]

Note: The efficiency and lifetime for battery will also change over time. For complete parameters, see Supplementary Table 5 in [25].

In the context of cross-country flow of electricity, Germany initially appears as a net electricity importer but also contributes significantly to exports. In 2020, exports accounted for 11% of its total electricity consumption. However, there's a year-on-year decline in Germany's electricity exports, indicating a decreasing role in Germany international power transmission as a storage mechanism.

Denmark, a wind-dominated country, shows a markedly smaller battery storage capacity than Germany, projected to reach 8 GWh by 2050. Both direct and indirect H₂ storage capacities in Denmark, except for fuel cells, are set to increase substantially from 2045, five years earlier than in Germany. Notably, Denmark, as a net electricity exporter, sees its output comprising 74% of its total electricity load from 2020 to 2050. In contrast, Italy, a country where solar energy is more prevalent, experiences irregular yearly variations in electricity transmission with other countries. Italy primarily depends on battery and indirect H₂ storage, opting forgoes direct H₂ storage. Interestingly, Italy's capacity of electrolyzers and Sabatier processes significantly exceeds that of Germany.

In summary, this section provides basic insights into the energy transition pathways of Denmark, Italy, and Germany up to 2050. A key similarity across these countries is the increasing penetration rate of renewable energy and the collective move away from fuel cells. Another important commonality is the early-stage reliance on cross-country electricity flow, playing a

pivotal role during the initial rapid decarbonization phase, before significant energy storage involvement. As the transition progresses, however, their approaches begin to diverge. Denmark shows a smaller battery storage capacity compared to Germany, yet both nations are significantly ramping up their 2 kinds of hydrogen storage capacities, with Denmark starting this increase five years earlier. Denmark also stands out as a major electricity exporter, with a substantial part of its output derived from renewable sources. Italy exhibits a different pattern, with a different in the variation of electricity transmission with other countries and a greater reliance on battery and indirect hydrogen storage solutions.

Regarding the scope of our subsequent analysis, we will narrow our focus to specific time frames for each type of energy storage based on the conclusion from this section. For battery storage, the analysis will concentrate on the period from 2030 to 2050. This timeframe is crucial as it marks the phase when battery storage is expected to play a more prominent role in the energy transition. For H₂ storage, our examination will be confined to the decade from 2040 to 2050, a critical period for the maturation and increased implementation of hydrogen-based energy solutions.

3.2. Quantitative Analysis: Economic Performance of Storage

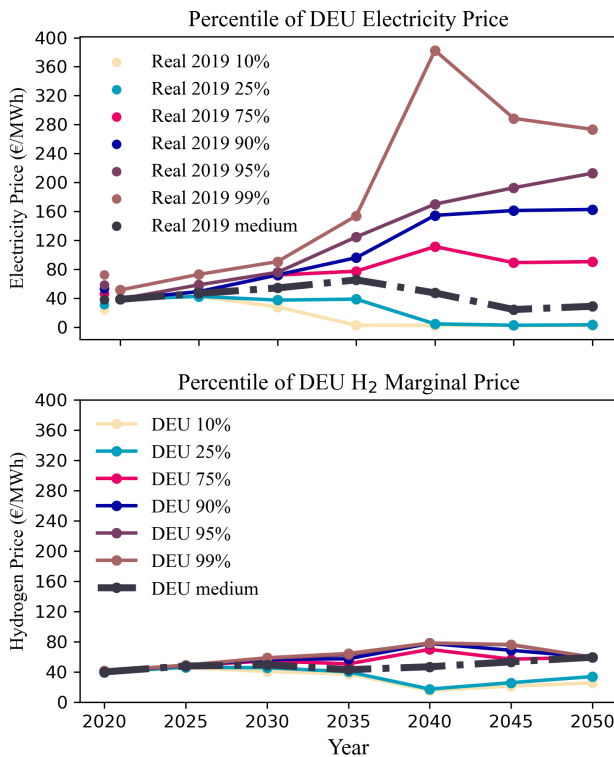


Figure 5. Historical and Projected Electricity Price and H₂ Marginal Price Distribution in Germany: A 2050 Outlook

In Figure 5, we illustrate the temporal evolution of electricity price percentiles and H₂ marginal price percentiles for Germany. For an extended comparative analysis involving Denmark and Italy, and for the distribution patterns of electricity

and H₂ marginal prices across these nations, we refer the readers to Appendix B supplementary figures S4, S5, and S6. The analysis of the electricity and H₂ price spread can provide a basis and reference for subsequent analysis of the energy storage benefits.

Figure 5 and Figure S4 indicates a common pattern among the three countries concerning electricity prices: a spreading of the price, denoted by the disparity between peak and trough values, which escalates progressively until 2040 before exhibiting a contraction. The median volatility of electricity prices maintains relative stability, with average fluctuations confined to below 53% for the countries in question. This stability, however, is not indicative of a clustering around the median price. Instead, it reflects a balance between the increasing occurrences of both high and low price extremes, as evidenced directly in Figure S4. Here, we observe a transition in electricity prices from a tight band of 25 €/MWh to 50 €/MWh to a broader distribution prior to 2040, subsequently reconverging but remaining more varied than in the baseline year of 2020. From 2020 to 2035, the disparity in electricity prices among Denmark, Germany, and Italy exhibited a remarkable similarity. However, future projections suggest a notable divergence in this trend. It is expected that from 2040, the electricity price differential in Denmark and Germany will converge and significantly exceed that of Italy. Specifically, the price spread in Denmark and Germany is projected to be 30% higher than in Italy during that year.

The spread of H₂ marginal prices is primarily influenced by fluctuations in electricity prices, given that hydrogen production is reliant solely on electrolysis. Notably, the spread of H₂ marginal prices exhibits an initial increase, peaking in 2040, before showing a decline. This trend is substantiated by Figure S5, which illustrates the H₂ marginal price shift from a narrow range of 20 €/MWh to 40 €/MWh to a broader distribution prior to 2040, followed by a convergence post-2040. While the distribution trends of H₂ marginal prices align with those of electricity prices, a notable shift in the relative positioning of H₂ marginal price spreads among the three countries has been observed. Contrasting with the behavior of electricity price spreads, projections from 2045 onwards indicate a reordering in the H₂ marginal price spreads. This new arrangement places Italy at the highest level, followed by Germany, and then Denmark, representing a significant deviation from electricity price spread trends. This inconsistency underscores that while electricity prices significantly influence H₂ marginal prices, they do not exclusively determine all facets of H₂ marginal prices.

In Figure 6, we present the dynamics of Germany storage buying and selling prices alongside electricity price distributions. In this analysis, the terms 'buying price' and 'selling price' refer to the electricity or H₂ prices at the specific times when the storage buys or sells energy. Therefore, the objective of Figure 6 is to examine the interplay between the buying and selling prices of energy storage, and the prices of electricity and H₂. Notably, the buying price for H₂ storage corresponds to the electricity price for powering electrolyzers, while the selling price is linked to the marginal price of H₂ as used in the Sabatier process. It's important to distinguish between two hydrogen

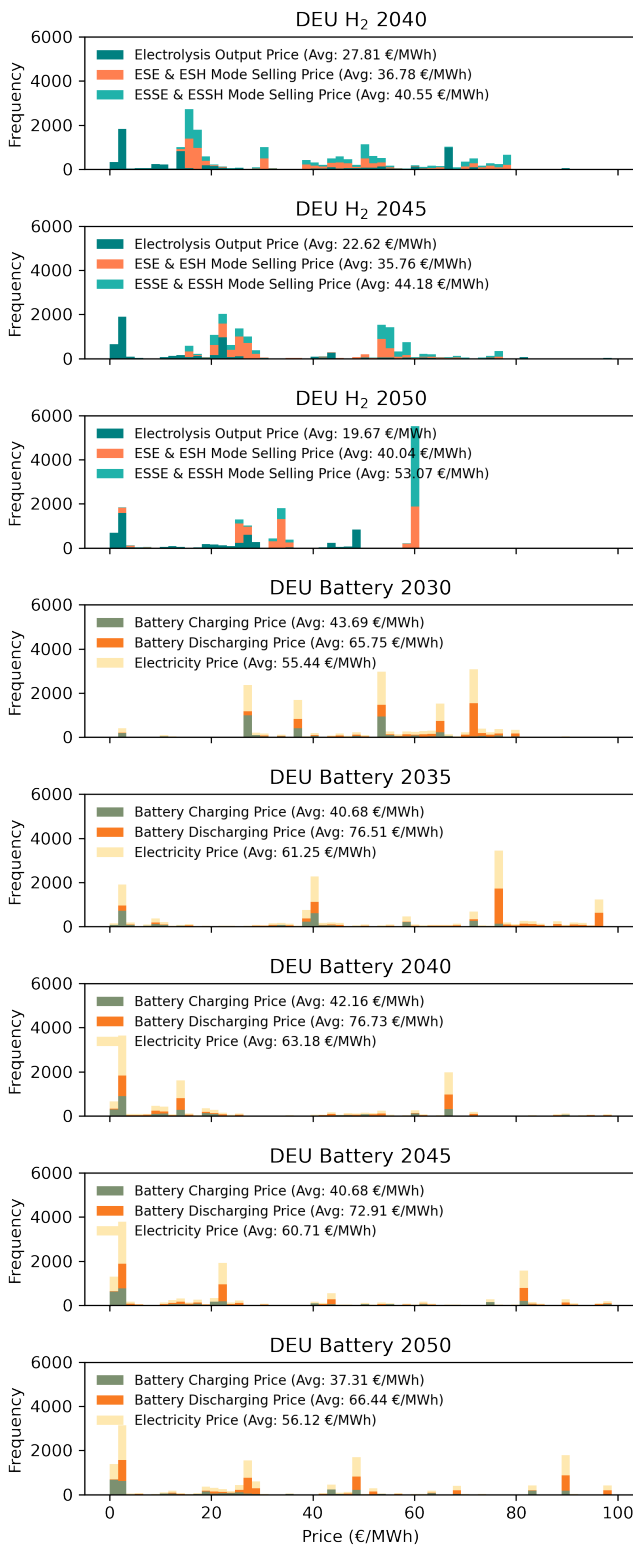


Figure 6. Comparative Price Distribution for Battery Storage Buying and Selling and Electricity (2030-2050) with Detailed Hydrogen Buying and Selling Analysis (2040-2050) in Germany

storage approaches: direct and indirect. Direct H₂ storage, as depicted here, excludes fuel cells, based on their infeasibility for energy transition demonstrated in Section 3.1. In contrast, for battery storage, the buying and selling prices directly reflect current electricity market rates. Figure 6 also integrates the battery buying and selling prices with the broader distribution of electricity prices. For detailed comparisons of storage pricing in Denmark and Italy, refer to Figure S7 in Appendix B.

In Figure 6, our observation reveals that in Germany, the buying price for energy from storage systems is typically lower, while the selling price is higher. The average selling price is lowest for energy selling from the indirect hydrogen storage, moderate for the direct hydrogen storage, and highest for battery storage. This pattern suggests the tank or underground H₂ storage from the direct hydrogen storage works well. Simply put, energy storage systems earn revenue by acquiring energy at a lower buying price and selling it at a higher selling price. Therefore, the gap between the lower energy prices and the higher energy prices becomes the main profit margin for energy storage. The difference in buying and selling prices across the three types of energy storage is in line with the trends in electricity and H₂ marginal price spreads observed in Figure 5, where the range of electricity price variation exceeds that of H₂ marginal price.

However, the largest average price difference among the three energy storage methods is seen in 2050. For indirect hydrogen storage, the maximum difference is 18 €/MWh, for direct hydrogen storage it's 24 €/MWh, and for battery storage, it reaches 38 €/MWh. This contrasts with the observation in Figure 5, where the peak spread difference between the two energy carrier is noted in 2040. In the cases of Denmark and Italy, as shown in Figure S7, a similar trend to Germany is observed. This indicates that energy prices are not the sole determinant of energy storage profit margins, and a more detailed investigation into the operational aspects of energy storage is warranted.

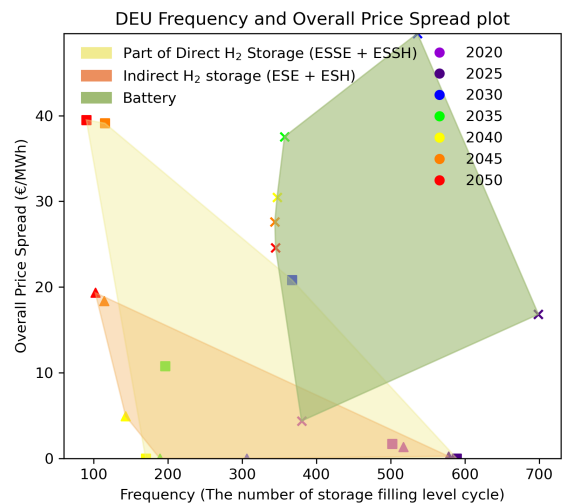


Figure 7. Analysis of Cycle Frequency and Overall Price Spreads in German H₂ Storage and Battery Systems (2020-2050)

Figure 7 presents the frequency (number of cycles) and overall price spread (OPS) of two types of hydrogen storage in Ger-

many (excluding ESFC working modes from direct H₂ storage due to fuel cell technology is unreliability under this study's assumptions) along with battery storage. The frequency is determined using the Cycle Capture (CC) Method. The OPS, also understood as the cycle-cased profitability index, quantifies the average difference in selling and buying prices within identified storage filling cycles over the year. For an in-depth explanation of OPS, see Equation 3. Thus, Figure 7 offers a detailed view of the operational dynamics of energy storage within the energy system, shedding light on the link between the profitability of energy storage, electricity prices, hydrogen price and the actual operation of energy storage. For a comparative analysis of hydrogen and battery storage performance in Denmark and Italy, refer to Figure S8 in Appendix B.

From Figure 7, we note that in the year marking Germany's shift to energy storage, the cycle frequencies for both indirect and direct H₂ storage were roughly 100 times per year, significantly lower than the battery storage cycle frequency, which was about 345 times per year. However, direct H₂ storage demonstrated the highest OPS, followed by battery storage, and then indirect H₂ storage. As shown in Figure S8, while the relative cycle frequencies of these energy storages remain consistent across the three countries, their OPS values vary in Denmark and Italy. In Denmark, direct H₂ storage's OPS is comparable to that of battery storage. In Italy, the OPS for indirect H₂ storage is similar to that of battery storage. It's also notable that the cycle frequencies for these three types of energy storage show considerable variation among the three countries. For direct and indirect H₂ storage, the frequency order from highest to lowest is Denmark, Germany, and Italy. For battery storage, the frequency order is reversed, with Denmark being the lowest and Italy the highest. This observation underscores how the actual operational practices of energy storage systems significantly affect their profitability, particularly in terms of storage charging and discharging frequencies and the associated price differences.

Figure 8 indicates the evolution of the cumulative leveled cost of storage (LCOS), unit benefit, and the installed capacities of hydrogen and battery storage systems in Germany. Each subplot is structured with dual y-axes: the left axis quantifies economic parameters, while the right axis measures the capacities of energy storage technologies. The initial subgraph of the analysis focuses on the German battery performance. Subsequently, the second subgraph examines all H₂ storage economic performance and direct H₂ storage capacity. The third subgraph addresses the economic performance and capacities of three hydrogen working modes associated with direct H₂ storage: Electrolysis - Store - Fuel Cell (ESFC), Electrolysis - Store - Sabatier - Electricity (ESSE), and Electrolysis - Store - Sabatier - Heating (ESSH). It is important to note that our model limited that the calculations for ESSE and ESSH modes cannot be separated on hour level but rather on an annual basis. Consequently, the LCOS and unit benefits for ESSE and ESSH are identical. A similar situation arises with the two indirect H₂ storage working modes: Electrolysis - Sabatier - Store - Electricity (ESE) and Electrolysis - Sabatier - Store - Heating (ESH), as demonstrated in the fourth subplot of our study. Notably, the measurement

of indirect H₂ storage capacity corresponds to the segment of the electrolyzer that supply energy directly to the Sabatier process, denominated in megawatts (MW). Conversely, the capacity of direct H₂ storage is measured by the volume of hydrogen that can be stored underground or within tanks, denominated in megawatt-hours (MWh).

To contextualize these findings within a broader European framework, Figure S9 offers a comprehensive comparison of these indicators across Denmark, Germany, and Italy. Complementarily, Figure S10 sheds light on the non-cumulative leveled cost of storage for the three countries. The term 'non-cumulative' herein implies that at each time step, the costs are appraised based on the current price levels, ignoring the integration of historical costs. In this model, the point where the LCOS and unit benefit meet in Figure S10 is important because it shows when the money spent on the technology has been made back, which could also indicate when we might expect to see more investment in the technology's capacity. This point highlights a limitation in the model we used for this study. To show the real costs involved in moving to new energy technologies, Figure 8 includes the past costs that have built up over time. Additionally, we've added Figure S10 in Appendix B to check that our findings are accurate.

In Germany, the convergence of the LCOS and the unit benefit for battery storage is projected to occur in 2035. This indicates that, from 2035 onwards, battery technology will start to provide economic value and its capacity is expected to increase substantially. However, a downward trend in unit benefits is detected from 2035 to 2050, with a decrease from the initial 40 €/MWh to 26 €/MWh. This trend deeper underscores the disconnect between the changes in energy storage economic performance and the fluctuations in electricity price spreads.

Regarding H₂ storage in Germany, it is not until 2050 that we foresee the LCOS aligning with the unit benefit, with a significant expansion in its capacity. The projected unit benefit for H₂ storage in 2050 is 21 €/MWh. When comparing the unit benefits of battery and H₂ storage, it's evident that although the former is higher, it also implies a greater investment per unit of energy. Focusing specifically on direct and indirect H₂ storage, their respective unit benefits in 2050 are anticipated to be 28.5 €/MWh and 18 €/MWh. It is also notable that most of the energy stored in both these forms of H₂ storage is likely to be towards the heating sector. This is evident from the fact that the capacities for ESSH and ESH are projected to be higher than those for ESSE and ESE, respectively.

In examining battery storage growth in Denmark, Germany, and Italy, we observe a simultaneous increase across these countries. By 2035, the unit benefits of battery storage are expected to outweigh their LCOS. Denmark exhibits the highest unit benefit and LCOS, followed by Germany, and then Italy with the lowest. This variation likely results from Italy's higher frequency of battery usage compared to Denmark's lower usage frequency, as evidenced in Figure 7 and Figure S21. Regarding storage capacity, Denmark, Germany, and Italy follow an ascending order. Remarkably, when comparing absolute values of battery storage capacity, Denmark's figures appear less significant, especially when shown alongside Germany's in Figure S9

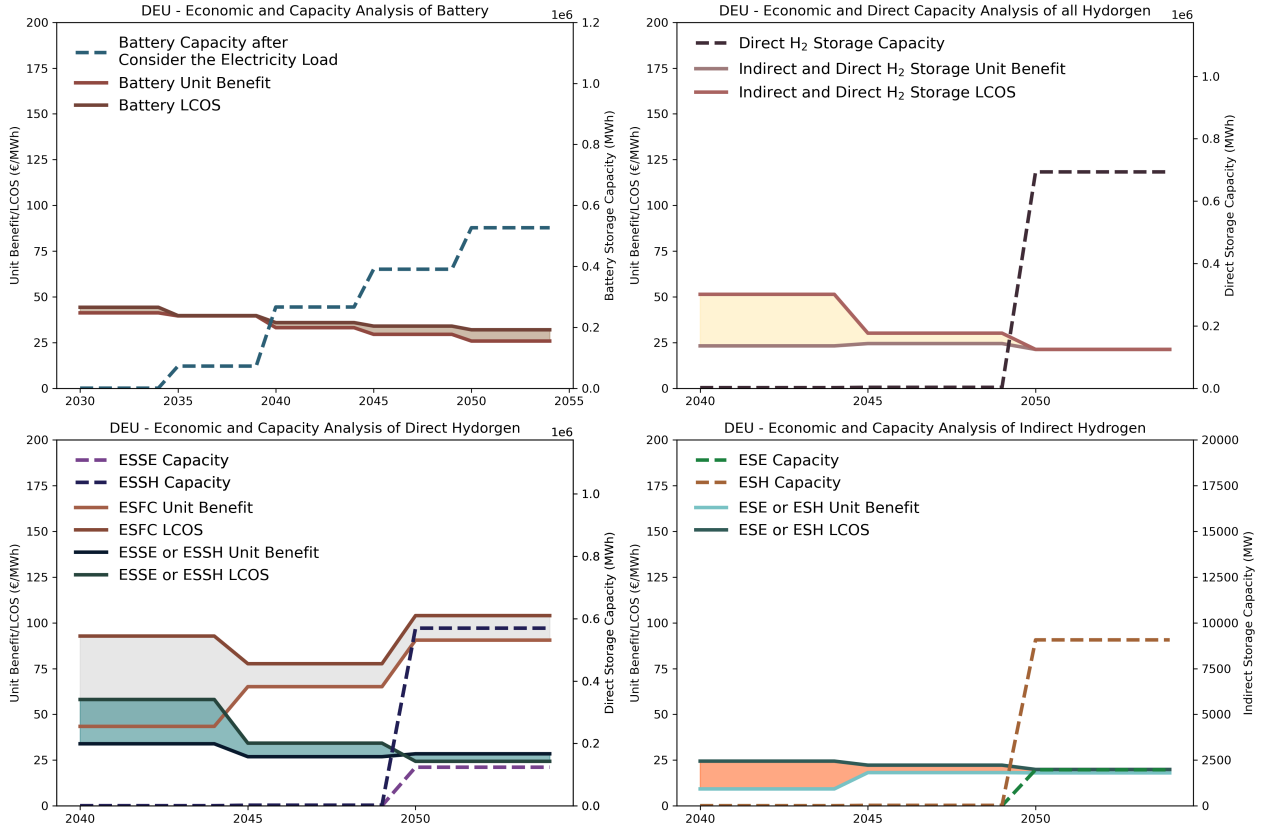


Figure 8. Temporal Evolution of LCOS, Unit Benefits, and Capacities of Energy storage in Germany in the Late Energy Transition Stage

and Figure S10. However, this comparison doesn't account for Denmark's substantially smaller electricity load, which is 16 times less than Germany's. By multiplying Denmark's capacity figures by 16, we can more accurately appreciate the extent of its expansion, highlighting the critical role of battery storage in a country heavily reliant on wind energy like Denmark.

In contrast, the dynamics of H₂ storage in these countries present a different picture. Denmark shows the lowest unit benefit and LCOS for H₂ storage, with Germany highest and Italy in between. This suggests that Italy finds building H₂ storage more appealing compared to Germany. Italy's preference for indirect H₂ storage over direct H₂ storage, due to the latter's inability to recover initial investments, is also notable. After accounting for the influence of electricity load, Italy's direct H₂ storage capacity still surpasses that of Germany. What's more, the ESFC plans in all three countries indicate that they are unlikely to recoup initial investments by 2050, explaining the lack of acceptance for these plans under this study's assumptions.

Figure 9 presents the revenue distribution of five hydrogen storage modes in Germany for the years 2040, 2045, and 2050. Focusing on the total revenue, we note a significant increase by 2050, reaching €2.2 billion. This figure is more than 99.7% higher than the total revenue in 2045, and even more so compared to 2040. In the year 2050, indirect H₂ storage contributes to 63.4% of Germany's total H₂ storage revenue, indicating its predominant role in revenue generation. Additionally, a notable aspect is that the majority of H₂, whether from indirect or direct

storage, is used in the heating sector, accounting for 82.1% of the revenue.

Similar patterns are observed in Denmark and Italy, as shown in Figure S11. Italy relies exclusively on indirect H₂ storage, while in Denmark, indirect H₂ storage comprises 75.3% of the total H₂ storage revenue. Remarkably, in 2050, Italy leads the three countries with a total revenue of €3.3 billion, followed by Denmark with €2.4 billion.

3.3. Qualitative Analysis: Time – Frequency Interdependency Analysis

In this section, we use Fast Fourier Transform (FFT), Continuous Wavelet Transform (CWT), and Cycle Capture (CC) methods to study changes in electricity prices, renewable energy generation, and energy storage filling levels in three different countries. Our study examines snapshot data at seven points, every five years from 2020 to 2050. The selected methodologies aim to accurately detect genuine fluctuations within the collected data, facilitating a more in-depth validation of the interaction among different segments of the energy system as inferred from these fluctuations. The variation in results from different volatility analysis methods does not imply inaccuracies in any method, rather, it highlights the unique focal points each method offers. And here, we're only showing Germany's electricity price fluctuation figure for 2020, 2030, 2040, and 2050 in the main body of the article, as shown in Figure 10.

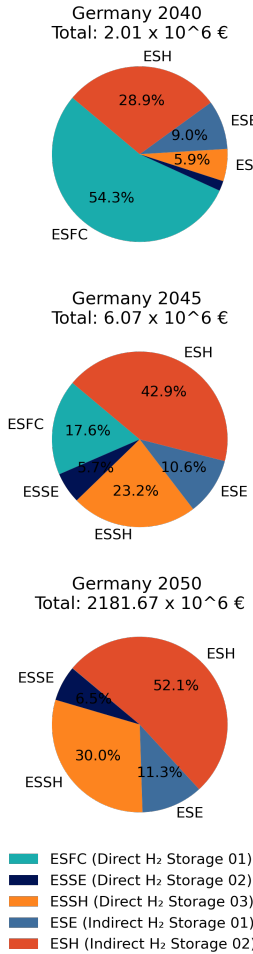


Figure 9. Revenue Distribution of Germany’s H₂ Storage Working Modes in 2040, 2045, and 2050

The Appendix B, specifically Figures S12 to S26, provides detailed data on the changes in electricity prices, renewable energy production, and levels of energy storage from 2020 to 2050 across three countries. This section will first examine the fluctuations in these areas separately, highlighting the real trends in each dataset. Then, we’ll connect these various pieces of information to understand the relationship among electricity prices, renewable energy generation and energy storage. It is worth to note that in the Cycle Capture method, we set the upper and lower boundaries for both renewable energy power generation and storage filling levels at 10% of their normalized values. For the electricity price, the limit was set at 5%.

Figure 10 presents varied analytical outcomes on electricity prices in Germany across four distinct years, derived from three different methods. The variation in results from different volatility analysis methods does not imply inaccuracies in any method, rather, it highlights the unique focal points each method offers. This section will first synthesize insights from all three methods to unveil the authentic fluctuations in the assorted data sets. Subsequently, this paper will interconnect these disparate data to create a link between electricity prices and the energy storage and renewable generation that have been

identified as key factors influencing electricity prices.

For the FFT analysis results of electricity prices, as displayed in Figure 10 and Figure S13. Denmark’s electricity prices fluctuated mainly on larger scales such as weekly, monthly, and seasonally. In Germany, fluctuations ranged widely from daily to seasonal scales. Italy saw changes mostly daily and seasonally. However, from 2040, price fluctuations became more evenly spread across all scales. The intensity of fluctuations at nearly all scales decreased, with Italy experiencing the most significant reduction, showing only minor dominant fluctuations daily and seasonally. Denmark was the least affected by this decrease.

The CWT depicted in Figure 10 and Figure S12 elucidates the temporal evolution of frequency components within the electricity prices for Denmark, Germany, and Italy. Commencing in 2040, robust seasonality is discernible across all three nations, aligning with the observations made via FFT. This seasonality is particularly pronounced on the seasonal scale from 2040 onwards. CWT, however, offers a more nuanced insight, revealing that the apparent surge in seasonality during this period is attributed to the attenuation of frequencies on shorter time scales during the summer months. Conversely, during the winter months, the frequency components on these shorter time scales are retained. A peculiar observation is noted for Italy, where the strength of seasonality peaks in 2040 and then experiences a gradual decline. The salience of frequencies across most scales seems to harmonize over time, yet distinctions in the seasonal and diurnal scales remain perceptible. And CWT results further proves what was said at the previous paragraph that the information or variability in the electricity prices is more evenly distributed across different frequency scales.

The CC analysis results, as presented in Figure 10 and Figure S14, reveal variations exceeding 5% in the electricity prices across three countries. First, these variations are predominantly observed on daily and weekly scales. This suggests that despite our focus on the larger-scale frequency components in the FFT and CWT, the short-term frequency components remain crucial throughout. They offer insights into the intricate dynamics of the energy system. Second, the annual trend of these fluctuations aligns with the annual variations in the FFT frequency component on daily and weekly scales. Predictions suggest that the frequency component of electricity prices in these countries, based on daily and weekly scales, will peak in 2030. This indicates the appropriateness of the parameter settings for electricity price changes in the CC analysis.

In summary the analysis of the electricity price across three countries, the patterns of frequency fluctuations in electricity prices vary among the three countries. Denmark primarily focuses on large time scale fluctuations, Germany considers fluctuations across all scales, while Italy mainly highlights those on a daily scale. The daily significance frequency of electricity prices in all three nations reaches its zenith in 2030. By 2040, frequencies start to spread uniformly across scales compare to before. This paper subsequently carried out same analysis for energy storage filling level and renewable energy generation using.

Next, we enter the analysis of energy storage filling level.

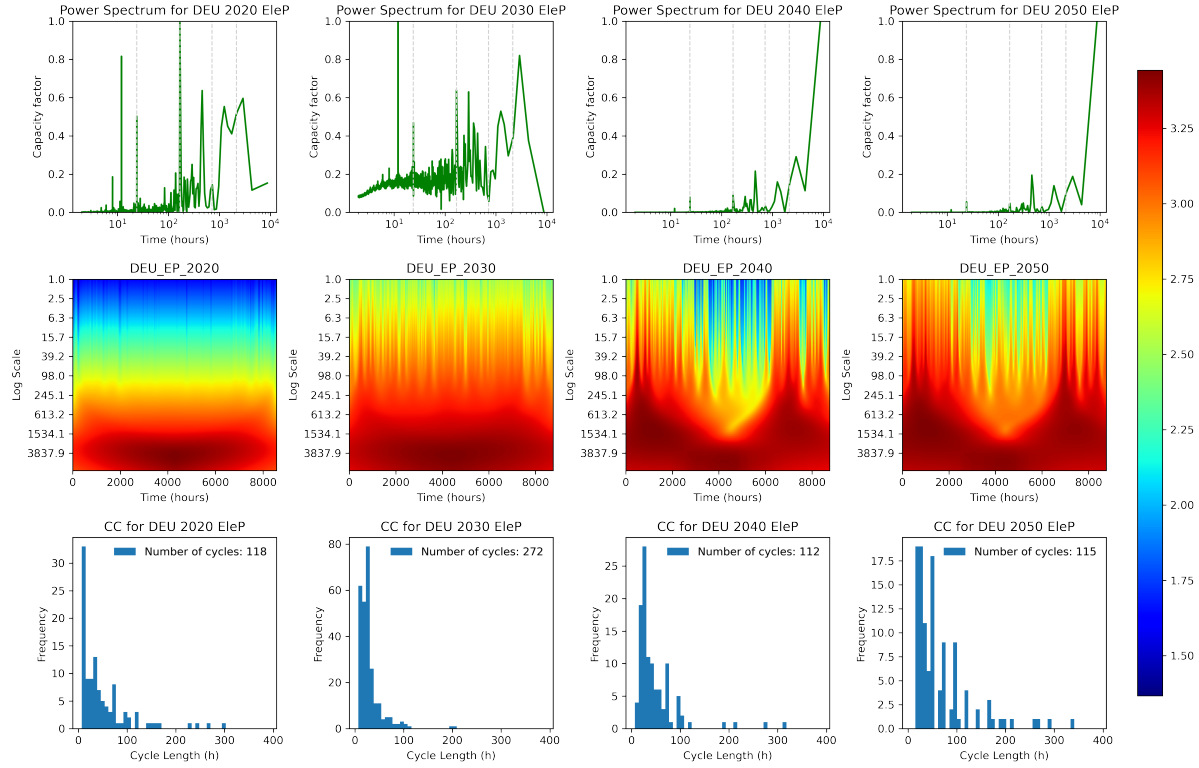


Figure 10. Wavelets, Cycles, and Spectra: Deciphering Germany’s Electricity Price Evolution in 2020, 2030, 2040 and 2050

Readers need to refer to Figures S15 to S21 in Appendix B. The battery filling levels, as depicted in Figures S15, S20, and S21, predominantly exhibit fluctuations on daily scale across all three examined countries. Notably, Denmark and Germany also exhibit fluctuations on a weekly scale, with Denmark showing a stronger tendency. Similar to electricity prices, daily scale fluctuations peak in 2030 as indicated by the CC results.

Distinct frequency characteristics are observed in the direct and indirect H₂ storage fluctuations across different countries, as delineated in Figures S15 to S19. Focusing on the direct H₂ storage fluctuations, we find that Italy, as our previous analysis, lacks direct H₂ storage capacity along its transition path. Therefore, our attention is directed towards Denmark and Germany. In these countries, the primary frequencies are predominantly around the monthly scale. The CC results show that charge and discharge energy fluctuations exceeding 10% still occur on a daily or weekly scale. Furthermore, the CWT analysis suggests that while clear seasonality is absent in the both countries, the frequency of direct H₂ storage on the short-period scale is gaining increasing prominence.

Regarding the performance of indirect H₂ storage fluctuations, a distinct different pattern emerges when compared to the direct H₂ storage. Interestingly, in the years when indirect H₂ storage became significant, its main fluctuation pattern matched exactly with that of electricity prices in size and intensity. Moreover, during summer, indirect H₂ storage displayed strong daily fluctuations, perfectly complementary with the changes in electricity prices. This indicates that indirect H₂ storage is effectively adjusting to the varying energy structures

of different countries.

For renewable energy generation, Figures S22 to S26 highlight that wind energy mainly fluctuates weekly, monthly, and seasonally, while solar energy fluctuates daily and seasonally. Before energy storage came into play, the fluctuations in electricity prices closely matched the patterns of renewable energy generation, significantly influencing price variability.

This section examines the volatility of electricity prices, renewable energy production, and energy storage levels using three methods, uncovering some possible connections. It’s important to consider these findings alongside those in section 3.1. This paper use the moment energy storage starts impacting the energy system as a key point to explore changes in electricity prices. Before 2040, fluctuations in electricity prices are largely driven by renewable energy volatility. Afterward, prices are influenced by how well renewable energy and energy storage balance out. Notably, the relationship between electricity prices and energy storage is mutual. While we only focus on how energy storage affects electricity prices in this section, it’s interesting to see that indirect H₂ storage adjusts its impact according to different energy systems, showing varying patterns of fluctuation. In contrast, battery storage and direct H₂ storage influence electricity prices on short-duration and long-duration bases, respectively.

4. Conclusions

Energy storage, renewable energy generation, and electricity prices in highly renewable Europe have been investigated

through a network of one node per country, which is resolved every hour of the European energy system and is aimed to achieve a 95% carbon reduction by 2050. From the data of 30 countries, three countries – Denmark, Germany, and Italy – with distinct climates, were chosen for a deeper examination. This article aims to elucidate the intricate dynamics within the energy system. To this end, it outlines five distinct H₂ working methodologies, classifying them into two categories: direct H₂ storage and indirect H₂ storage. This paper delves into the energy system's complexities from both quantitative and qualitative perspectives.

The article outlines specific strategies for the energy transition in Denmark, Germany, and Italy, setting the stage for our analysis. Initially, energy storage didn't contribute to the quick reduction of carbon emissions in these countries, with international electricity transmission adding flexibility to their energy systems. Fuel cell technology was set aside by all three countries due to cost concerns—it needs to be more affordable to be considered a feasible option for the energy transition. Renewable energy's impact on the energy system was fixed, shaping electricity price fluctuations before the introduction of energy storage. Once energy storage came into play, electricity prices began to reflect the balance between renewable energy and the different types of energy storage.

It's important to note the two-way relationship between electricity prices and energy storage. From the perspective of how electricity prices affect energy storage, the spread of prices is a major source of profit for energy storage solutions. However, the profitability of energy storage also depends on the specific energy structure of a location, which influences how it operates. On the other hand, looking at how energy storage affects electricity prices, each of the three energy storage methods uniquely reduces price fluctuations by leveraging different patterns. Among these, indirect H₂ storage stands out as a common choice in all three countries, thanks to its better economic performance and its ability to adapt flexibly to various energy structures. In Denmark, battery storage faces capacity constraints, and Italy has moved away from direct H₂ storage. These developments further underline the crucial role of indirect H₂ storage in advancing the transition to cleaner energy.

CRediT authorship contribution statement

Zhiyuan Xie: Writing – review & editing, Writing – original draft, Visualization, Validation, Coding, Methodology, Investigation, Formal analysis, Conceptualization. **Gorm Bruun Andresen:** Writing – review & editing, Supervision, Methodology, Funding acquisition, Conceptualization.

Declaration of generative Ai in scientific writing

During the preparation of this work, the authors used OpenAI in order to generate some icons for Figure 1. After using this tool, the authors reviewed and edited the content as needed and takes full responsibility for the content of the publication.

Acknowledgements

Zhiyuan Xie gratefully acknowledges the financial support received from the China Scholarship Council. Gorm Bruun Andresen is funded by the GridScale project supported by the Danish Energy Technology Development and Demonstration Program, Denmark under grant number 64020-2120. Special thanks are extended to Dr. Sleiman Farah, Mr. Ebbe Kyhl Gøtske, and colleagues from the author's focus group for their invaluable assistance with this paper. Appreciation is also due to Miss Fang Fang for her skillful assistance in plotting Figures 1 and 2.

Declaration of competing interest

The authors declare that they have no known competing financial interests or personal relationships that could have appeared to influence the work reported in this paper.

Data availability

The datasets used as input as well as the data generated by the model have been indicated in the paper.

Code availability

The code about model and plot have been indicated in the paper.

Appendix A. Key Formulations in PyPSA-Eur-Sec-30 Model

The PyPSA-Eur-Sec-30-path model jointly optimizes the capacity and dispatch of each asset, including generation, storage, and transmission capacities. This optimization is done under assumptions of perfect foresight, competition, and long-term market equilibrium. Built within the Python for Power System Analysis (PyPSA) framework, the model determines the optimal system configuration by minimizing the total annualized system cost.

$$\min_{\substack{G_{n,s}, E_{n,s}, \\ F_l, G_{n,s,t}, F_l}} \left[\sum_{n,s} C_{n,s} \cdot G_{n,s} + \sum_{n,s} \varepsilon_{n,s} \cdot E_{n,s} \right. \\ \left. + \sum_l C_l \cdot F_l + \sum_{n,s,t} O_{n,s,t} \cdot G_{n,s,t} \right] \quad (\text{S1})$$

Here, the equation represents the total annualized cost, which is the sum of all costs associated with power and storage capacity, energy storage capacity, bus connectors, and the variable costs of operation across all buses, storage technologies, and time periods. n means the different buses, s means the different technologies, t means the time and resolution is 1h, l include transmission line and converters between the buses implemented in every country (node).

Victoria *et al.*[31] has identified three potential pathways to decarbonization: linear, a gradual start followed by rapid progression (exponential decay path), and a rapid start followed by a gradual approach (beta distribution path). The latter—beginning swiftly and then slowing down—is considered the best. This paper analysis will directly base on the best path and is as follows:

$$e(t) = e_0(1 - CDF_\beta(t)) \quad (\text{S2})$$

$$CDF_\beta(t) = \int_{t_0}^t PDF_\beta(t) dt \quad (\text{S3})$$

$$PDF_\beta(t) = \frac{\Gamma(2\beta)}{2\Gamma(\beta)^2} (t - t_0)^{\beta-1} (t_f - t)^{\beta-1} \quad (\text{S4})$$

In 2020, carbon emissions from electricity generation and the heating supply in Europe's residential and service sectors were 1.56 GtCO₂, constituting 43.5% of total European emissions. For the future, the carbon budget for these sectors in Europe is determined to be 21 GtCO₂. This budget is estimated in the context of a global carbon budget of 800 GtCO₂, which is the threshold to prevent temperature increases above 1.75C relative to the preindustrial era with a probability exceeding 66% [45]. The integral from the base year t_0 extending into the future of $e(t)$ is set to equal this carbon budget B , $\int_{t_0}^{\infty} e(t) dt = B$. That will mean we have a CO₂ emission cap for each time step.

This optimization process also should subject to various constraints, and among these constraints, the match of the supply and demand is the most important.

$$\sum_s G_{n,s,t} + \sum_l a_{n,l,t} \cdot f_{l,t} = d_{n,t} \leftrightarrow \lambda_{n,t} \quad \forall n, t \quad (\text{S5})$$

In the energy system model, $\lambda_{n,t}$ represents the Karush-Kuhn-Tucker (KKT) multiplier. When equilibrium is achieved in the electricity bus, this multiplier reflects the locational marginal price (LMP), which is the price of electricity at that specific node.

Appendix B. Supplementary Figures

The following pages present a series of Supplementary Figures, numbered S1 through S25. Each figure is provided on a separate page for clarity and detailed examination.

References

- [1] R. Mutschler, M. Rüdisüli, P. Heer, S. Eggimann, Benchmarking cooling and heating energy demands considering climate change, population growth and cooling device uptake, *Applied Energy* 288 (2021) 116636. doi:[10.1016/j.apenergy.2021.116636](https://doi.org/10.1016/j.apenergy.2021.116636).
- [2] A. Aghahosseini, A. Solomon, C. Breyer, T. Pregger, S. Simon, P. Strachan, A. Jäger-Waldau, Energy system transition pathways to meet the global electricity demand for ambitious climate targets and cost competitiveness, *Applied energy* 331 (2023) 120401. doi:[10.1016/j.apenergy.2022.120401](https://doi.org/10.1016/j.apenergy.2022.120401).
- [3] J. Gea-Bermúdez, I. G. Jensen, M. Münster, M. Koivisto, J. G. Kirkerud, Y.-k. Chen, H. Ravn, The role of sector coupling in the green transition: A least-cost energy system development in northern-central europe towards 2050, *Applied Energy* 289 (2021) 116685. doi:[10.1016/j.apenergy.2021.116685](https://doi.org/10.1016/j.apenergy.2021.116685).
- [4] R. Li, B.-J. Tang, B. Yu, H. Liao, C. Zhang, Y.-M. Wei, Cost-optimal operation strategy for integrating large scale of renewable energy in china's power system: From a multi-regional perspective, *Applied Energy* 325 (2022) 119780. doi:[10.1016/j.apenergy.2022.119780](https://doi.org/10.1016/j.apenergy.2022.119780).
- [5] G. Ren, J. Wan, J. Liu, D. Yu, Spatial and temporal assessments of complementarity for renewable energy resources in china, *Energy* 177 (2019) 262–275. doi:[10.1016/j.energy.2019.04.023](https://doi.org/10.1016/j.energy.2019.04.023).
- [6] A. Gangopadhyay, A. K. Seshadri, B. Patil, Wind-solar-storage trade-offs in a decarbonizing electricity system, *Applied Energy* 353 (2024) 121994. doi:doi.org/10.1016/j.apenergy.2023.121994.
- [7] O. Erixno, N. A. Rahim, F. Ramadhan, N. N. Adzman, Energy management of renewable energy-based combined heat and power systems: A review, *Sustainable Energy Technologies and Assessments* 51 (2022) 101944. doi:[10.1016/j.seta.2021.101944](https://doi.org/10.1016/j.seta.2021.101944).
- [8] H. Wang, W. Yin, E. Abdollahi, R. Lahdelma, W. Jiao, Modelling and optimization of chp based district heating system with renewable energy production and energy storage, *Applied Energy* 159 (2015) 401–421. doi:[10.1016/j.apenergy.2015.09.020](https://doi.org/10.1016/j.apenergy.2015.09.020).
- [9] A. Q. Al-Shetwi, Sustainable development of renewable energy integrated power sector: Trends, environmental impacts, and recent challenges, *Science of The Total Environment* 822 (2022) 153645. doi:[10.1016/j.scitotenv.2022.153645](https://doi.org/10.1016/j.scitotenv.2022.153645).
- [10] X. Liang, Emerging power quality challenges due to integration of renewable energy sources, *IEEE Transactions on Industry Applications* 53 (2) (2016) 855–866. doi:[10.1109/TIA.2016.2626253](https://doi.org/10.1109/TIA.2016.2626253).
- [11] S. Borenstein, The private and public economics of renewable electricity generation, *Journal of Economic Perspectives* 26 (1) (2012) 67–92. doi:[10.1257/jep.26.1.67](https://doi.org/10.1257/jep.26.1.67).
- [12] P. L. Joskow, Comparing the costs of intermittent and dispatchable electricity generating technologies, *American Economic Review* 101 (3) (2011) 238–241. doi:[10.1257/aer.101.3.238](https://doi.org/10.1257/aer.101.3.238).
- [13] J. M. Gonzalez, J. E. Tomlinson, E. A. Martínez Ceseña, M. Basheer, E. Obuobie, P. T. Padi, S. Addo, R. Baisie, M. Etichia, A. Hurford, et al., Designing diversified renewable energy systems to balance multisector performance, *Nature Sustainability* 6 (2023) 415–427. doi:[10.1038/s41893-022-01033-0](https://doi.org/10.1038/s41893-022-01033-0).
- [14] X. Fang, H. Cui, E. Du, F. Li, C. Kang, Characteristics of locational uncertainty marginal price for correlated uncertainties of variable renewable generation and demands, *Applied Energy* 282 (2021) 116064. doi:[10.1016/j.apenergy.2020.116064](https://doi.org/10.1016/j.apenergy.2020.116064).
- [15] A. Biber, M. Felder, C. Wieland, H. Spliethoff, Negative price spiral caused by renewables? electricity price prediction on the german market for 2030, *The Electricity Journal* 35 (8) (2022) 107188. doi:[10.1016/j.tej.2022.107188](https://doi.org/10.1016/j.tej.2022.107188).
- [16] K. De Vos, Negative wholesale electricity prices in the german, french and belgian day-ahead, intra-day and real-time markets, *The Electricity Journal* 28 (4) (2015) 36–50. doi:[10.1016/j.tej.2015.04.001](https://doi.org/10.1016/j.tej.2015.04.001).
- [17] Z. Shao, Q. Zheng, C. Liu, S. Gao, G. Wang, Y. Chu, A feature extraction-and ranking-based framework for electricity spot price forecasting using a hybrid deep neural network, *Electric Power Systems Research* 200 (2021) 107453. doi:[10.1016/j.epsr.2021.107453](https://doi.org/10.1016/j.epsr.2021.107453).
- [18] A. Solomon, D. M. Kammen, D. Callaway, The role of large-scale energy storage design and dispatch in the power grid: a study of very high grid penetration of variable renewable resources, *Applied Energy* 134 (2014) 75–89. doi:[10.1016/j.apenergy.2014.07.095](https://doi.org/10.1016/j.apenergy.2014.07.095).
- [19] M. McPherson, N. Johnson, M. Strubegger, The role of electricity storage and hydrogen technologies in enabling global low-carbon energy transitions, *Applied Energy* 216 (2018) 649–661. doi:[10.1016/j.apenergy.2018.02.110](https://doi.org/10.1016/j.apenergy.2018.02.110).
- [20] M. Gimeno-Gutiérrez, R. Lacal-Arántegui, Assessment of the european potential for pumped hydropower energy storage based on two existing reservoirs, *Renewable Energy* 75 (2015) 856–868. doi:[10.1016/j.renene.2014.10.068](https://doi.org/10.1016/j.renene.2014.10.068).
- [21] Y. Scholz, H. C. Gils, R. C. Pietzcker, Application of a high-detail energy system model to derive power sector characteristics at high wind and solar shares, *Energy Economics* 64 (2017) 568–582. doi:[10.1016/j.eneco.2016.06.021](https://doi.org/10.1016/j.eneco.2016.06.021).
- [22] F. Cebulla, T. Naegler, M. Pohl, Electrical energy storage in highly renewable european energy systems: Capacity requirements, spatial distribution, and storage dispatch, *Journal of Energy Storage* 14 (2017) 211–223. doi:[10.1016/j.est.2017.10.004](https://doi.org/10.1016/j.est.2017.10.004).
- [23] O. Schmidt, S. Melchior, A. Hawkes, I. Staffell, Projecting the future levelized cost of electricity storage technologies, *Joule* 3 (1) (2019) 81–100. doi:[10.1016/j.joule.2018.12.008](https://doi.org/10.1016/j.joule.2018.12.008).
- [24] M. Victoria, K. Zhu, T. Brown, G. B. Andresen, M. Greiner, The role of storage technologies throughout the decarbonisation of the sector-coupled european energy system, *Energy Conversion and Management* 201 (2019) 111977. doi:[10.1016/j.enconman.2019.111977](https://doi.org/10.1016/j.enconman.2019.111977).
- [25] E. K. Gøtske, G. B. Andresen, M. Victoria, Cost and efficiency requirements for successful electricity storage in a highly renewable european energy system, *PRX Energy* 2 (2) (2023) 023006, publisher: American Physical Society. doi:[10.1103/PRXEnergy.2.023006](https://doi.org/10.1103/PRXEnergy.2.023006).
- [26] T. Brown, D. Schlachtberger, A. Kies, S. Schramm, M. Greiner, Synergies of sector coupling and transmission reinforcement in a cost-optimised, highly renewable european energy system, *Energy* 160 (2018) 720–739. doi:[10.1016/j.energy.2018.06.222](https://doi.org/10.1016/j.energy.2018.06.222).
- [27] H. Iranmehr, R. Aazami, J. Tavoozi, M. Shirkhani, A.-R. Azizi, A. Mohammadzadeh, A. H. Mosavi, W. Guo, Modeling the price of emergency power transmission lines in the reserve market due to the influence of renewable energies, *Frontiers in Energy Research* 9 (2022). doi:[10.3389/fenrg.2021.792418](https://doi.org/10.3389/fenrg.2021.792418).
- [28] J.-J. Shen, C.-t. Cheng, Z.-b. Jia, Y. Zhang, Q. Lv, H.-x. Cai, B.-c. Wang, M.-f. Xie, Impacts, challenges and suggestions of the electricity market for hydro-dominated power systems in china, *Renewable Energy* 187 (2022) 743–759. doi:[10.1016/j.renene.2022.01.089](https://doi.org/10.1016/j.renene.2022.01.089).
- [29] D. P. Schlachtberger, T. Brown, S. Schramm, M. Greiner, The benefits of cooperation in a highly renewable european electricity network, *Energy* 134 (2017) 469–481. doi:[10.1016/j.energy.2017.06.004](https://doi.org/10.1016/j.energy.2017.06.004).
- [30] K.-K. Cao, T. Pregger, J. Haas, H. Lens, To prevent or promote grid expansion? analyzing the future role of power transmission in the european energy system, *Frontiers in Energy Research* 8 (2021). doi:[10.3389/fenrg.2020.541495](https://doi.org/10.3389/fenrg.2020.541495).
- [31] M. Victoria, K. Zhu, T. Brown, G. B. Andresen, M. Greiner, Early decarbonisation of the european energy system pays off, *Nature communications* 11 (1) (2020) 1–9. doi:[10.1038/s41467-020-20015-4](https://doi.org/10.1038/s41467-020-20015-4).
- [32] K. Poncelet, E. Delarue, D. Six, W. D'haeseleer, Myopic optimization models for simulation of investment decisions in the electric power sector, in: 2016 13th International Conference on the European Energy Market (EEM), IEEE, 2016, pp. 1–9. doi:[10.1109/EEM.2016.7521261](https://doi.org/10.1109/EEM.2016.7521261).
- [33] A. Sgobbi, W. Nijs, R. De Miglio, A. Chiodi, M. Gargiulo, C. Thiel, How far away is hydrogen? its role in the medium and long-term decarbonisation of the european energy system, *International Journal of Hydrogen Energy* 41 (1) (2016) 19–35. doi:[10.1016/j.ijhydene.2015.09.004](https://doi.org/10.1016/j.ijhydene.2015.09.004).
- [34] M. Parzen, F. Neumann, A. H. Van Der Weijde, D. Friedrich, A. Kiprakis, Beyond cost reduction: improving the value of energy storage in electricity systems, *Carbon Neutrality* 1 (1) (2022) 26. doi:[10.1007/s43979-022-00027-3](https://doi.org/10.1007/s43979-022-00027-3).
- [35] S. Zhu, W. Ma, Research of power harmonic detection based on fft and wavelet transform, in: 2011 International Conference on Electrical and Control Engineering, IEEE, 2011, pp. 1177–1180. doi:[10.1109/ICECENG.2011.6057860](https://doi.org/10.1109/ICECENG.2011.6057860).
- [36] J. A. Rodenas, R. Garello, Wavelet analysis in sar ocean image profiles for internal wave detection and wavelength estimation, *IEEE Transactions on Geoscience and Remote Sensing* 35 (4) (1997) 933–945. doi:[10.1109/36.602535](https://doi.org/10.1109/36.602535).

- [37] A. B. Stepanov, Construction of activation functions for wavelet neural networks, in: 2017 XX IEEE International Conference on Soft Computing and Measurements (SCM), IEEE, 2017, pp. 397–399. doi: 10.1109/SCM.2017.7970597.
- [38] T. Guo, T. Zhang, E. Lim, M. Lopez-Benitez, F. Ma, L. Yu, A review of wavelet analysis and its applications: Challenges and opportunities, *IEEE Access* 10 (2022) 58869–58903. doi:10.1109/ACCESS.2022.3179517.
- [39] K. Zhu, M. Victoria, T. Brown, G. B. Andresen, M. Greiner, Impact of CO₂ prices on the design of a highly decarbonised coupled electricity and heating system in europe, *Applied Energy* 236 (2019) 622–634. doi: 10.1016/j.apenergy.2018.12.016.
- [40] C. Winterscheid, J.-O. Dalenbäck, S. Holler, Integration of solar thermal systems in existing district heating systems, *Energy* 137 (2017) 579–585. doi:10.1016/j.energy.2017.04.159.
- [41] Danish Energy Agency, Technology data – generation of electricity and district heating, Tech. rep. (2019). URL <https://ens.dk/en/our-services/projections-and-models/technology-data/technology-data-generation-electricity-and>
- [42] E. Vartiainen, G. Masson, C. Breyer, D. Moser, E. Román Medina, Impact of weighted average cost of capital, capital expenditure, and other parameters on future utility-scale pv levelised cost of electricity, *Progress in photovoltaics: research and applications* 28 (6) (2020) 439–453. doi: 10.1002/pip.3189.
- [43] E. Vartiainen, G. Masson, C. Breyer, The true competitiveness of solar pv: a european case study, in: Proceedings of the Annual Conference of the European Technology and Innovation Platform Photovoltaics-PV Manufacturing in Europe,(ETIP PV), Brussels, Belgium, 2017, pp. 18–19. doi:10.13140/RG.2.2.31543.93602.
- [44] C. Budischak, D. Sewell, H. Thomson, L. Mach, D. E. Veron, W. Kemp-ton, Cost-minimized combinations of wind power, solar power and electrochemical storage, powering the grid up to 99.9% of the time, *Journal of Power Sources* 225 (2013) 60–74. doi:10.1016/j.jpowsour.2012.09.054.
- [45] Intergovernmental Panel on Climate Change (IPCC), Global warming of 1.5 k, Tech. rep. (2018). URL <https://www.ipcc.ch/sr15/>

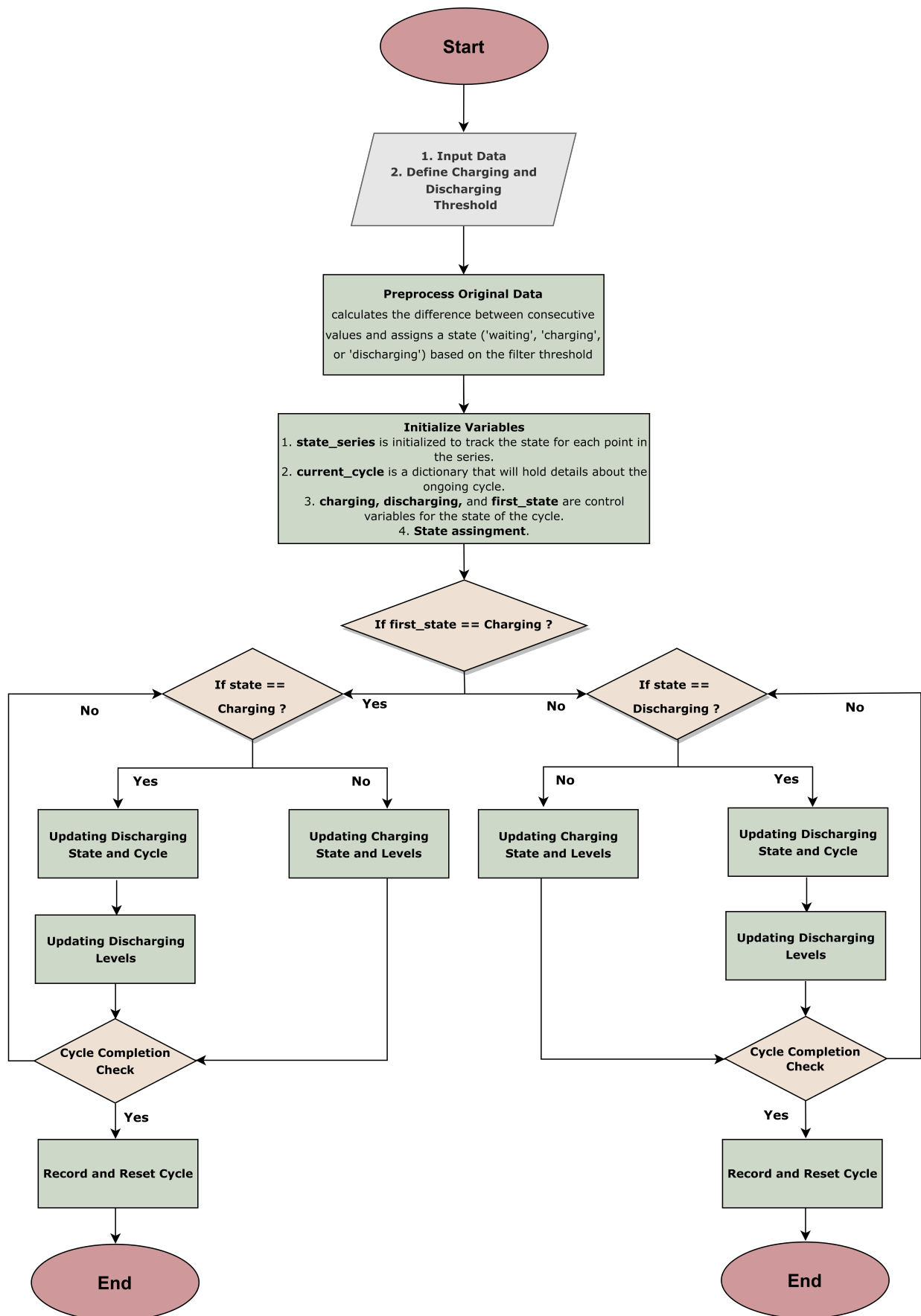


Figure S1. Operation Logic of Cycle Capture Method

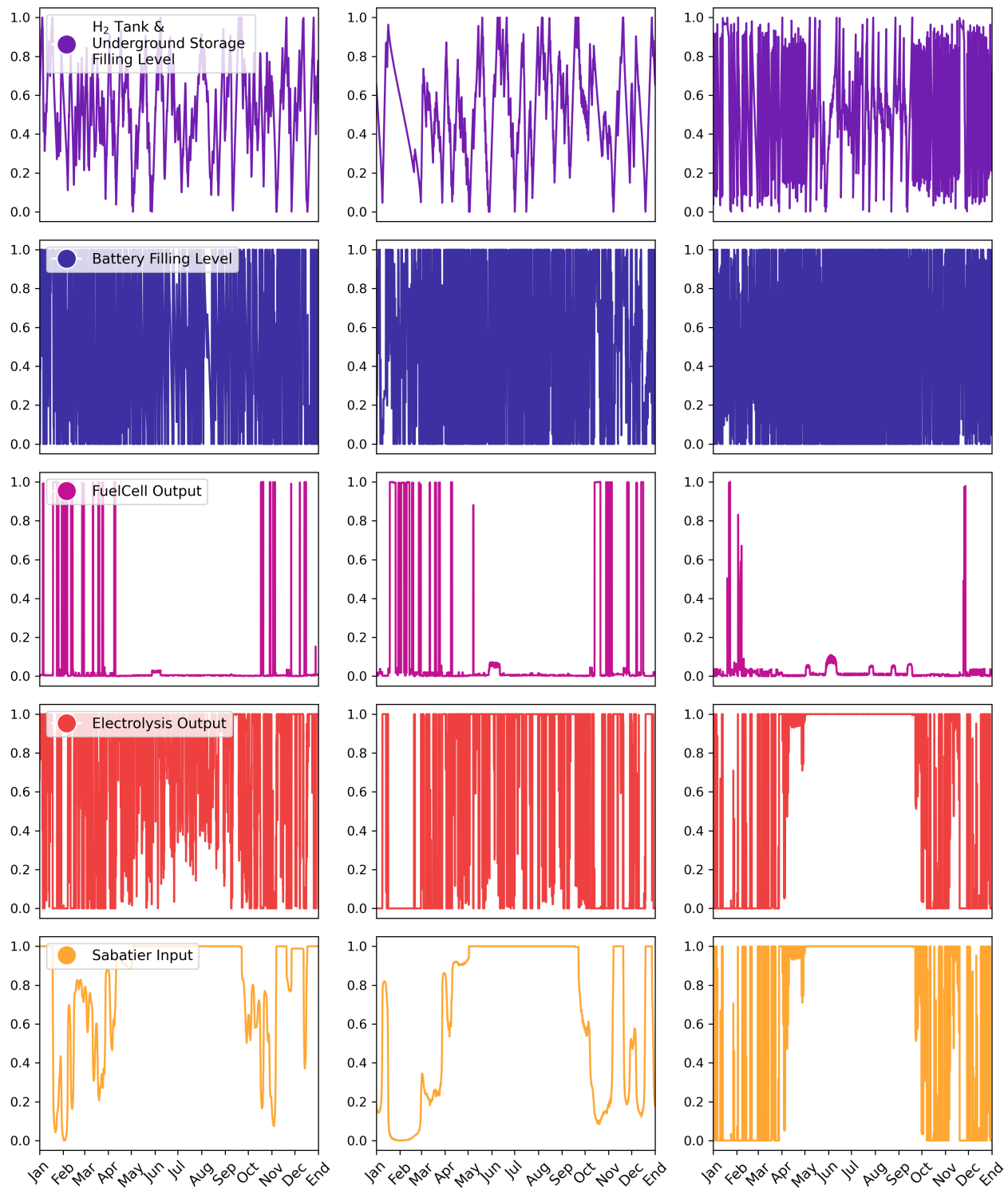


Figure S2. Time Series Analysis of Denmark, Germany and Italy Hydrogen Sector and Battery Storage for 2050

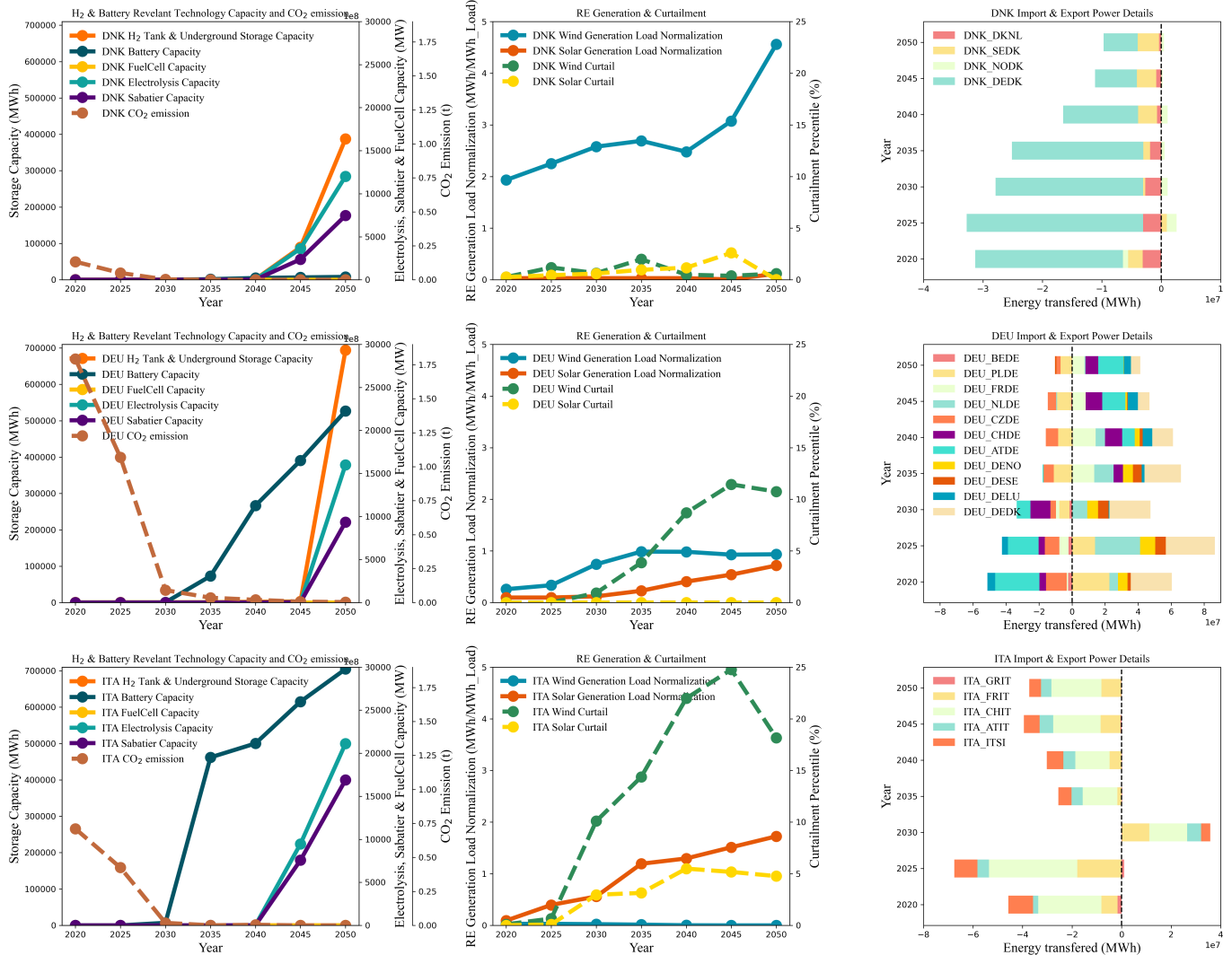


Figure S3. Evolution of Renewable Energy Landscapes in Denmark, Germany, and Italy: Capacity, Generation, Penetration, Cross-country Flow of Electricity, and CO₂ Emissions (2020-2050)

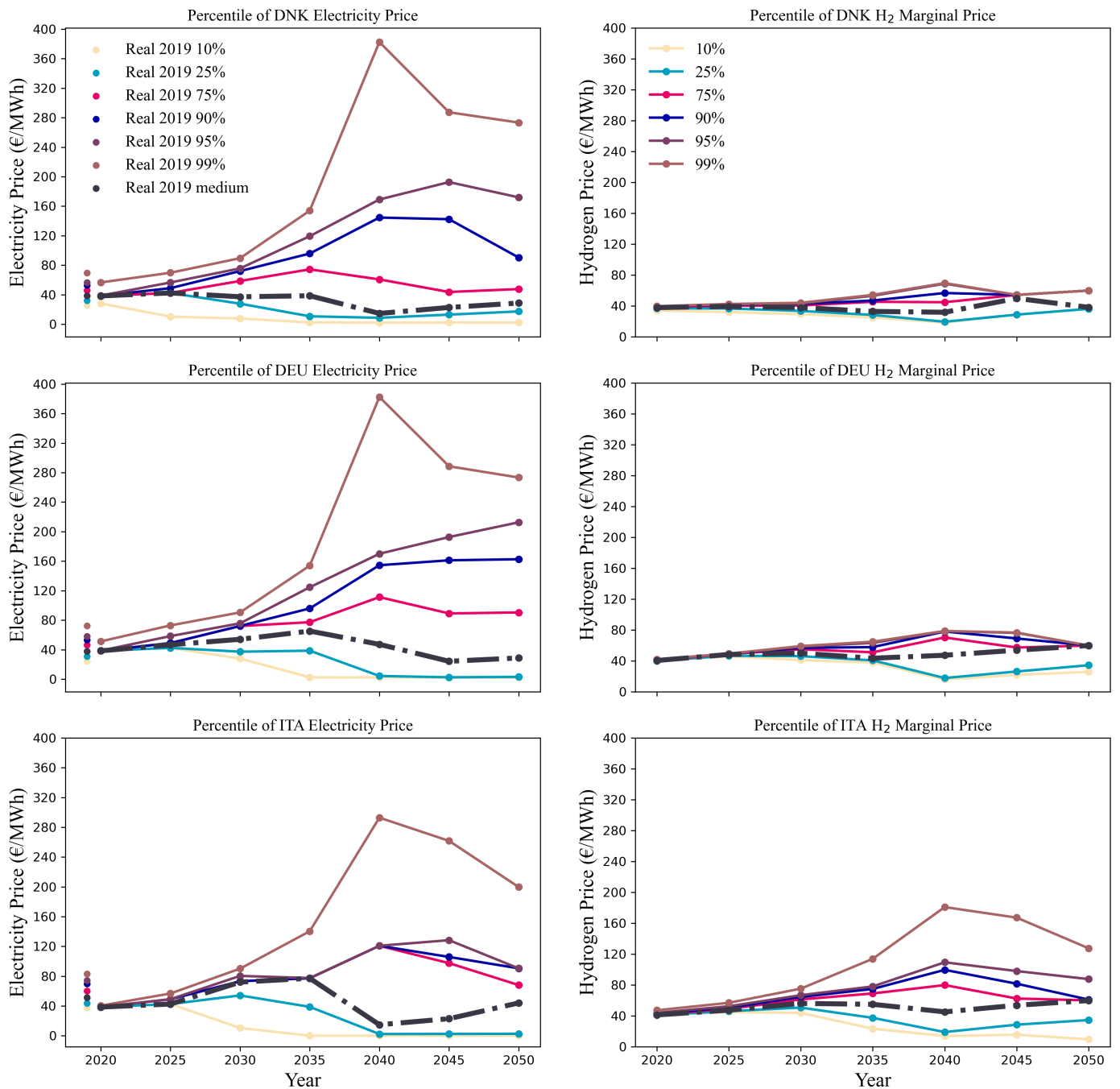


Figure S4. Historical and Projected Electricity Price Percentiles in Denmark, Germany, and Italy: A 2050 Outlook

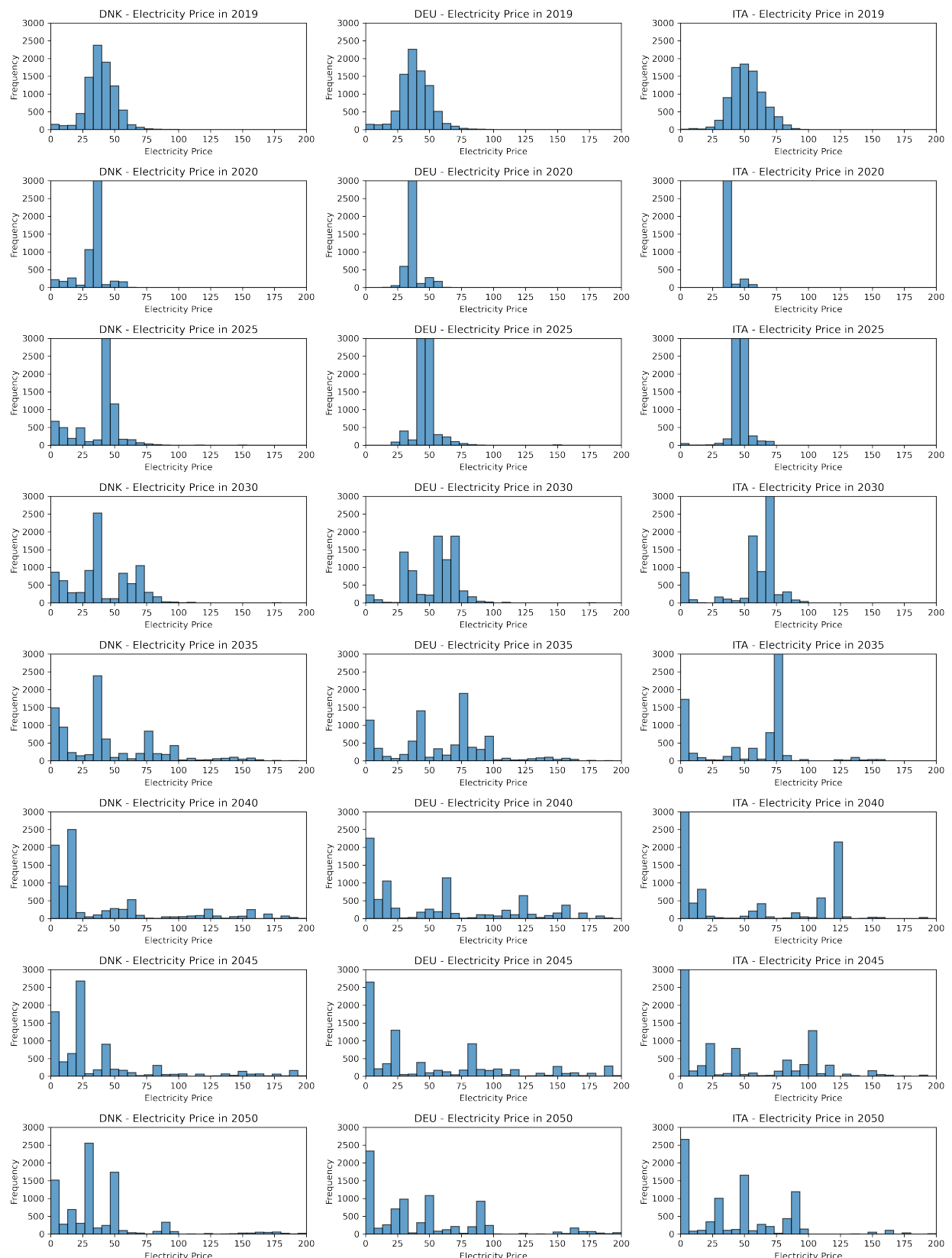


Figure S5. Historical and Projected Electricity Price Distribution in Denmark, Germany, and Italy: A 2050 Outlook

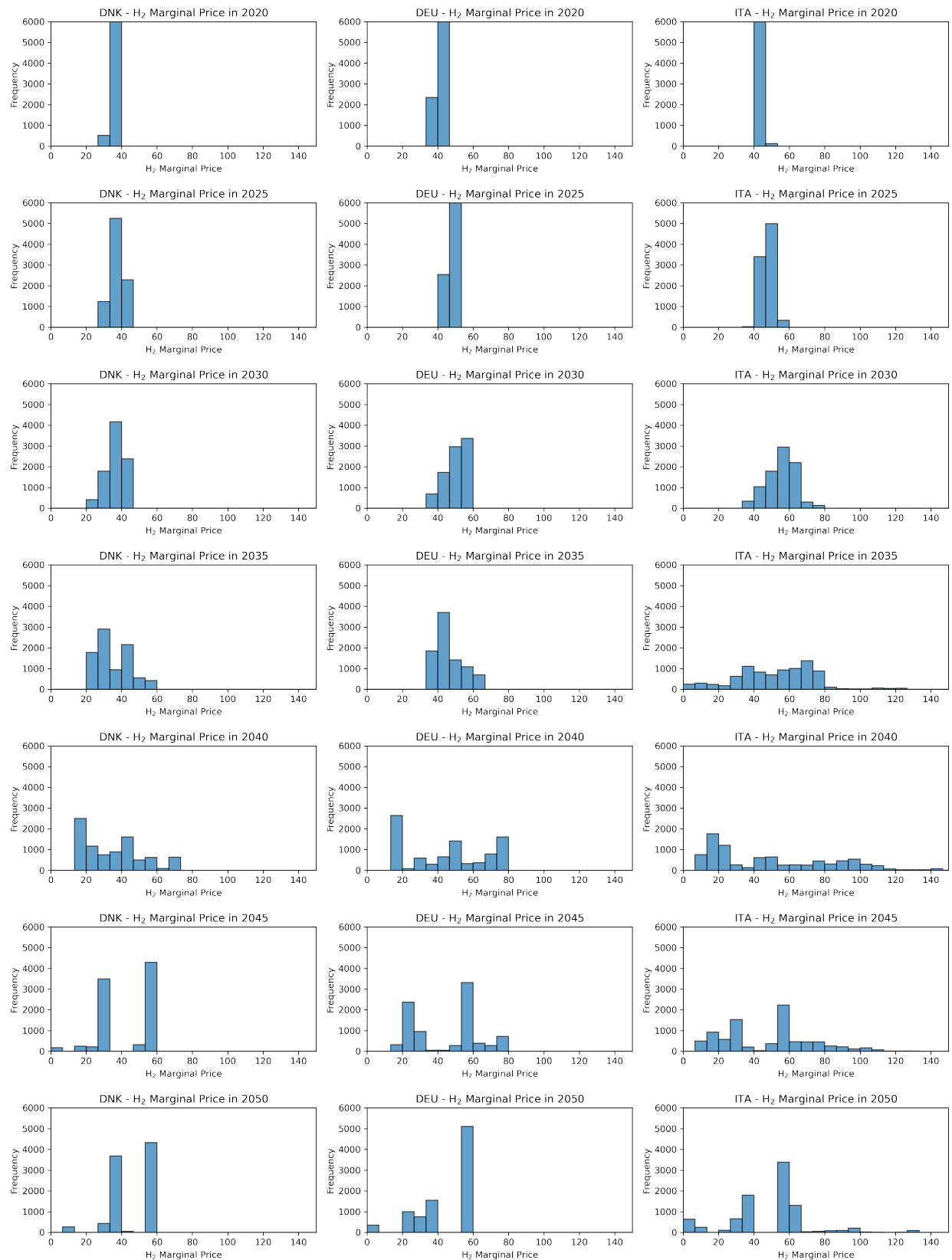


Figure S6. Historical and Projected H₂ Marginal Price Distribution in Denmark, Germany, and Italy: A 2050 Outlook

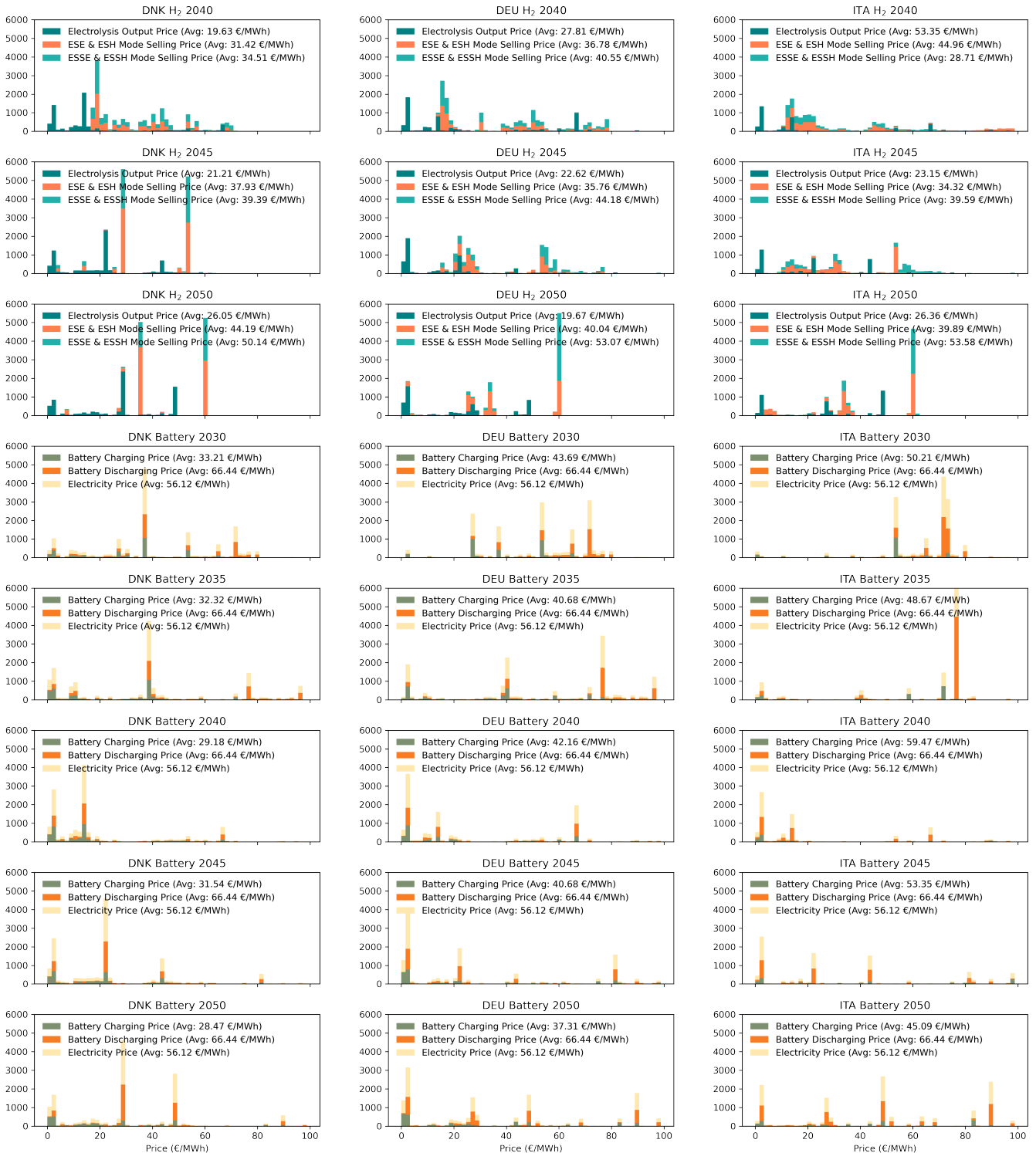


Figure S7. Comparative Price Distribution for Battery Storage Buying and Selling and Electricity (2030-2050) with Detailed Hydrogen Buying and Selling Analysis (2040-2050) in Denmark, Germany, and Italy

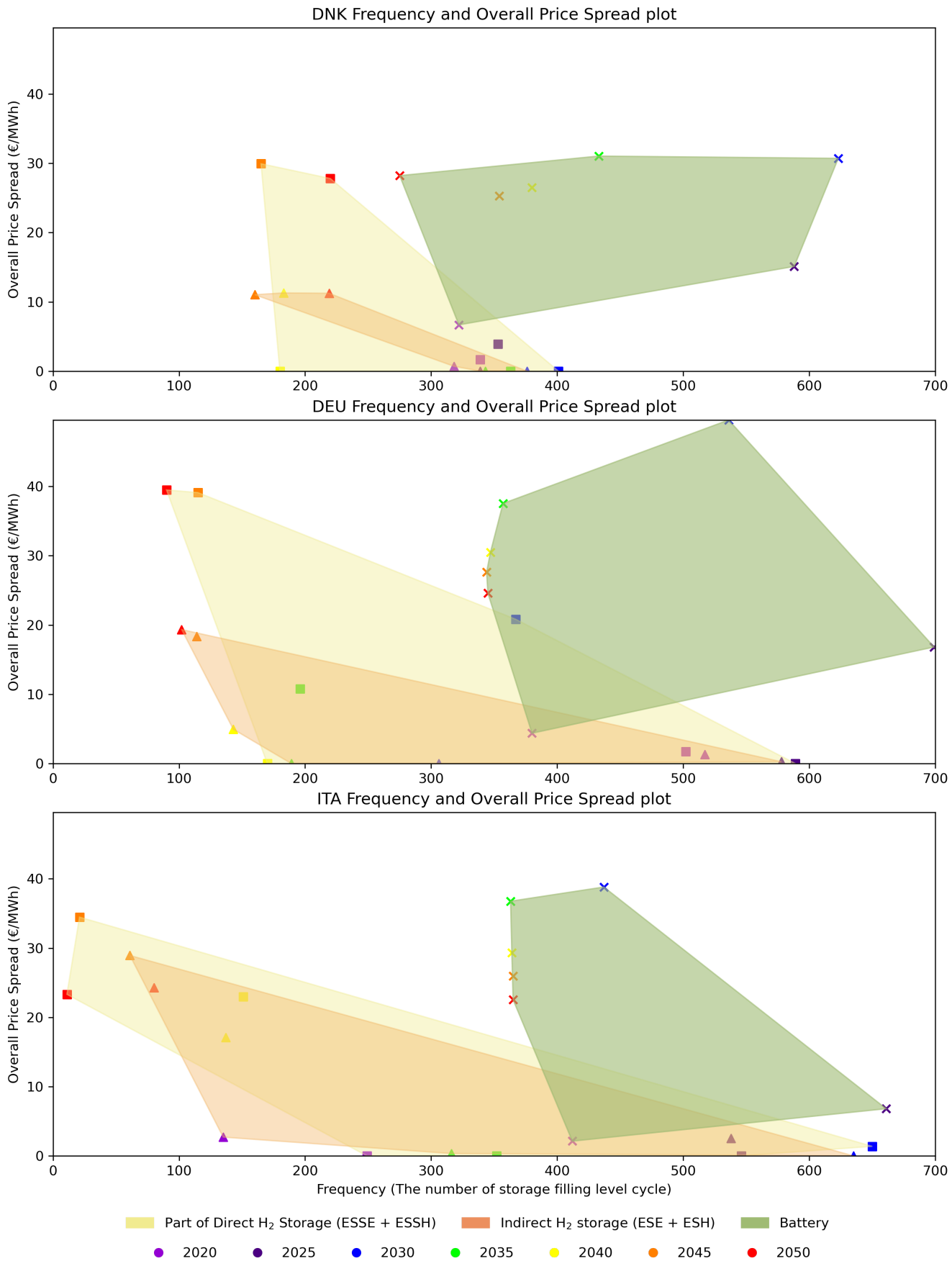


Figure S8. Comparative Performance of H₂ and Battery Systems in Denmark and Italy

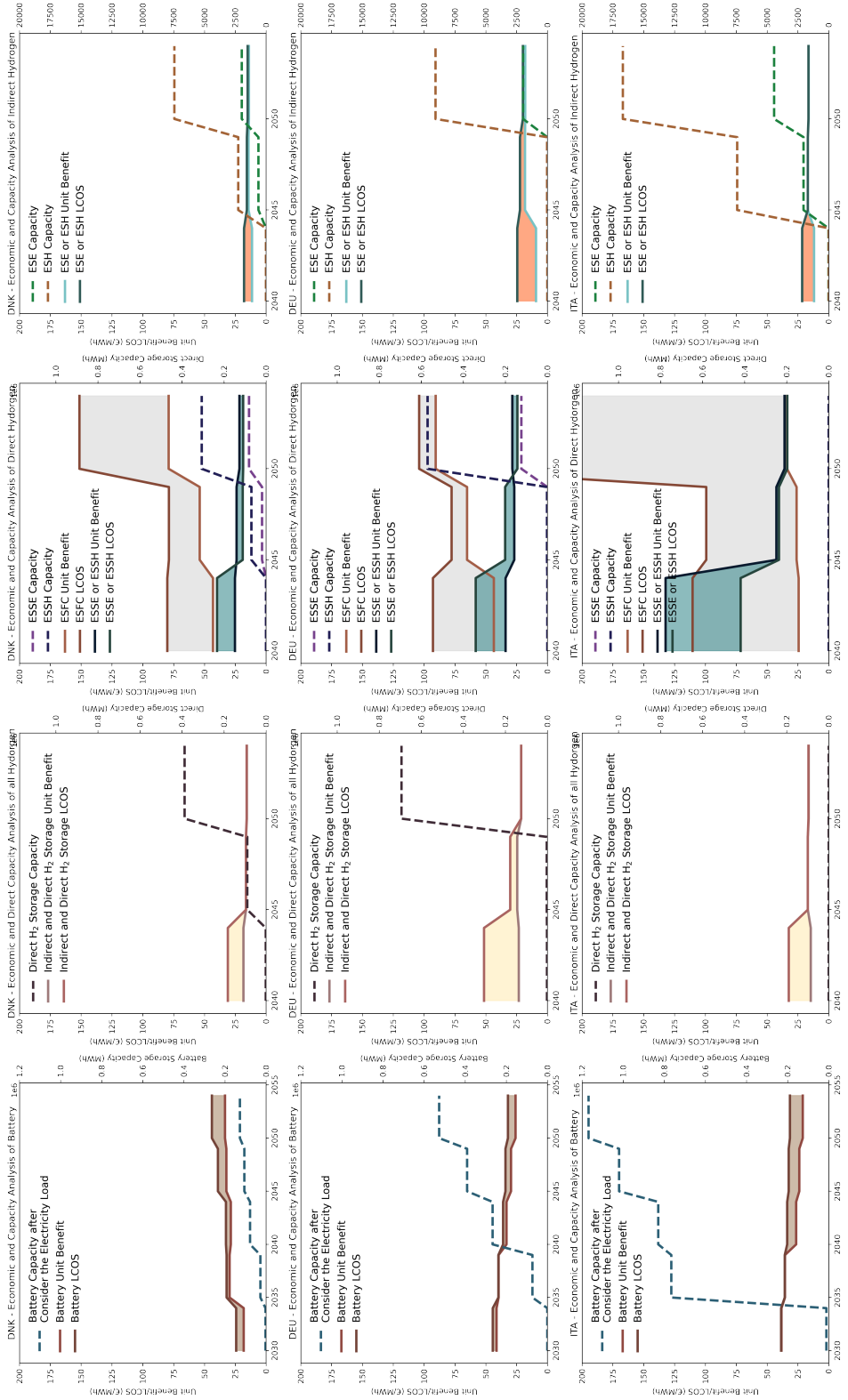


Figure S9. Projected Trends in Accumulated LCOS, Unit Benefits, and Capacities for Hydrogen and Battery Storage in Denmark, Germany, and Italy in the Late Energy Transition Stage

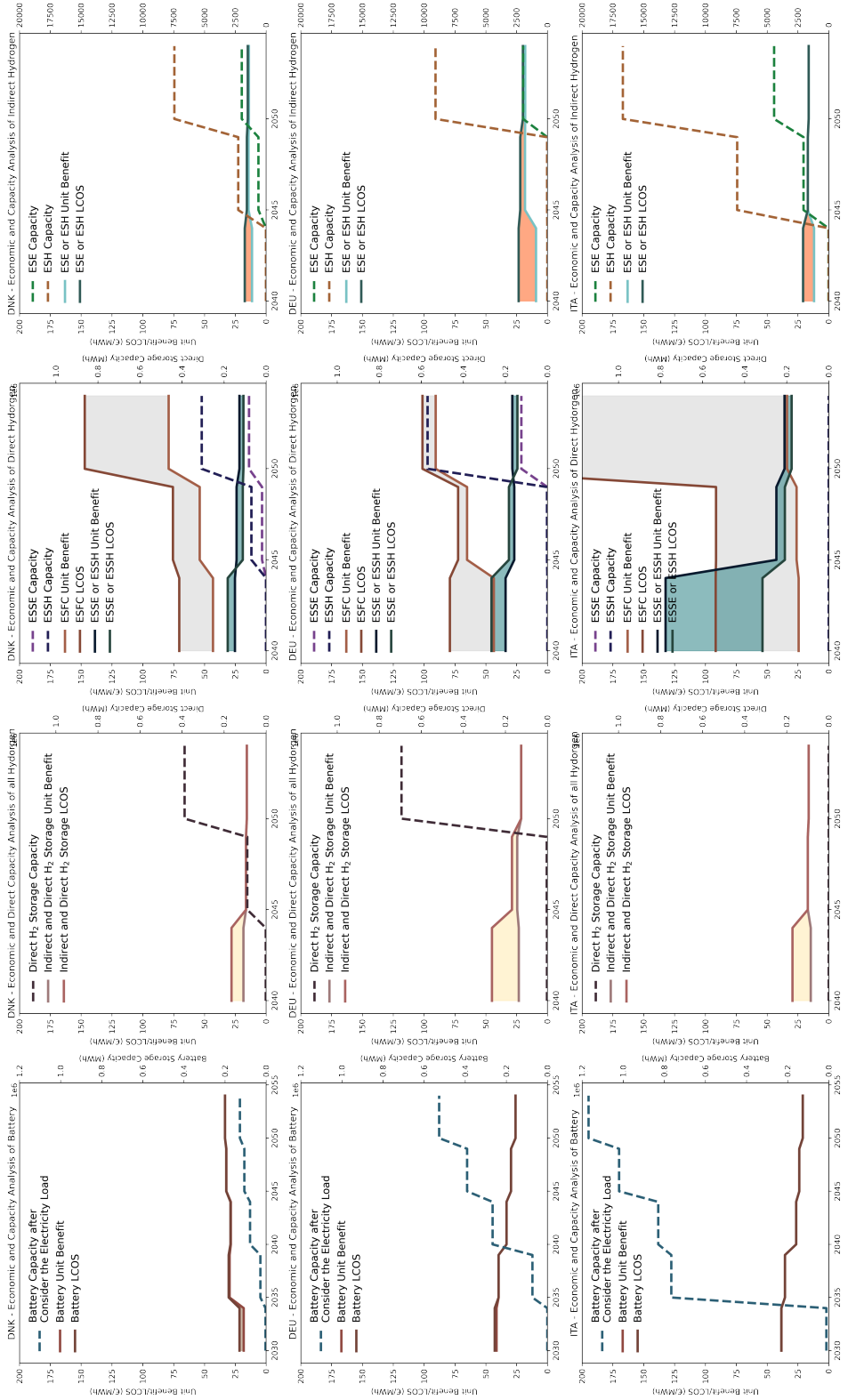


Figure S10. Comparative Analysis of Non-Accumulated LCOS for Hydrogen and Battery Storage in Denmark, Germany, and Italy in the Late Energy Transition Stage

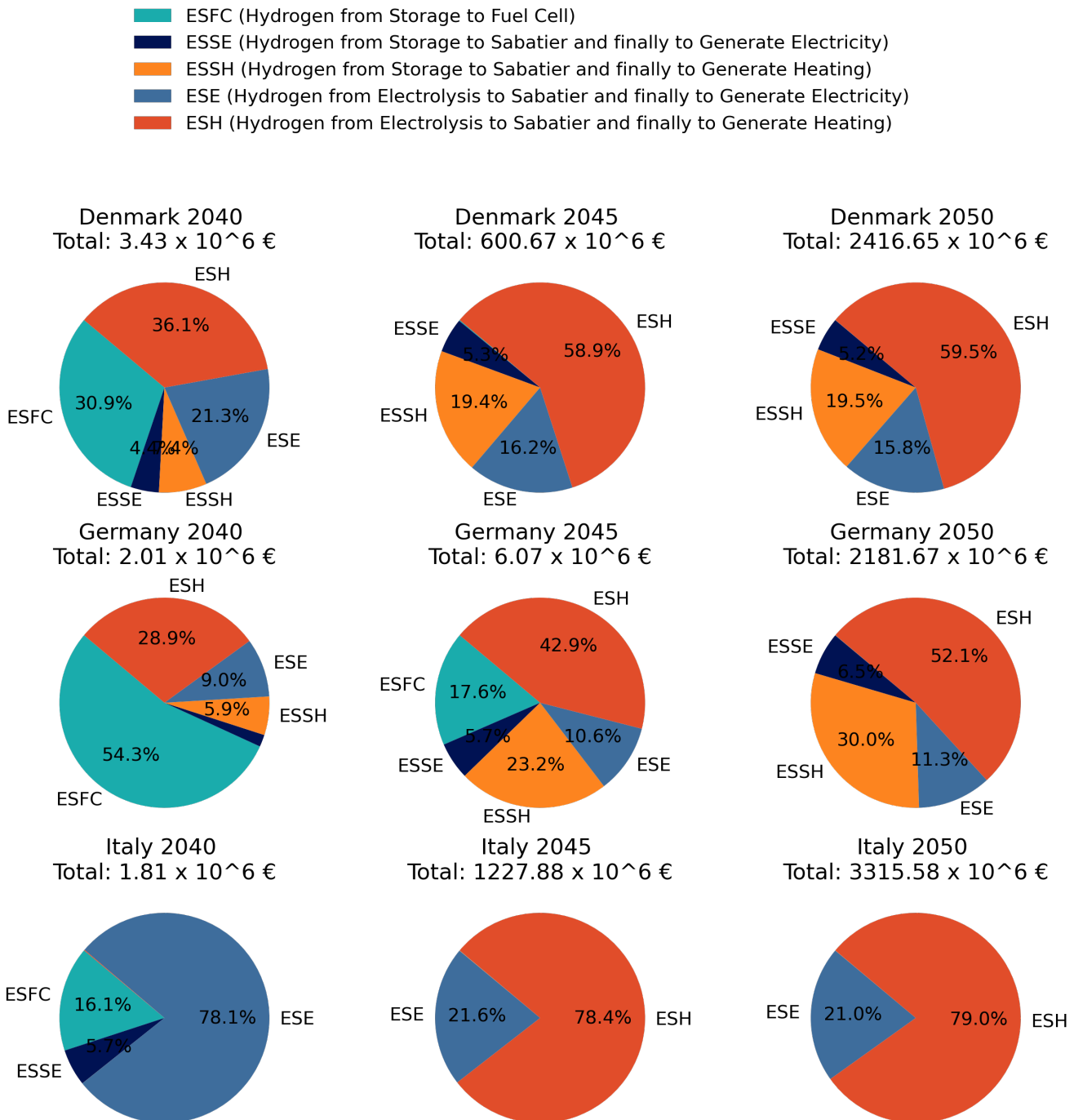


Figure S11. Revenue Distribution of Denmark, Germany and Italy H₂ Storage Working Modes in 2040, 2045, and 2050

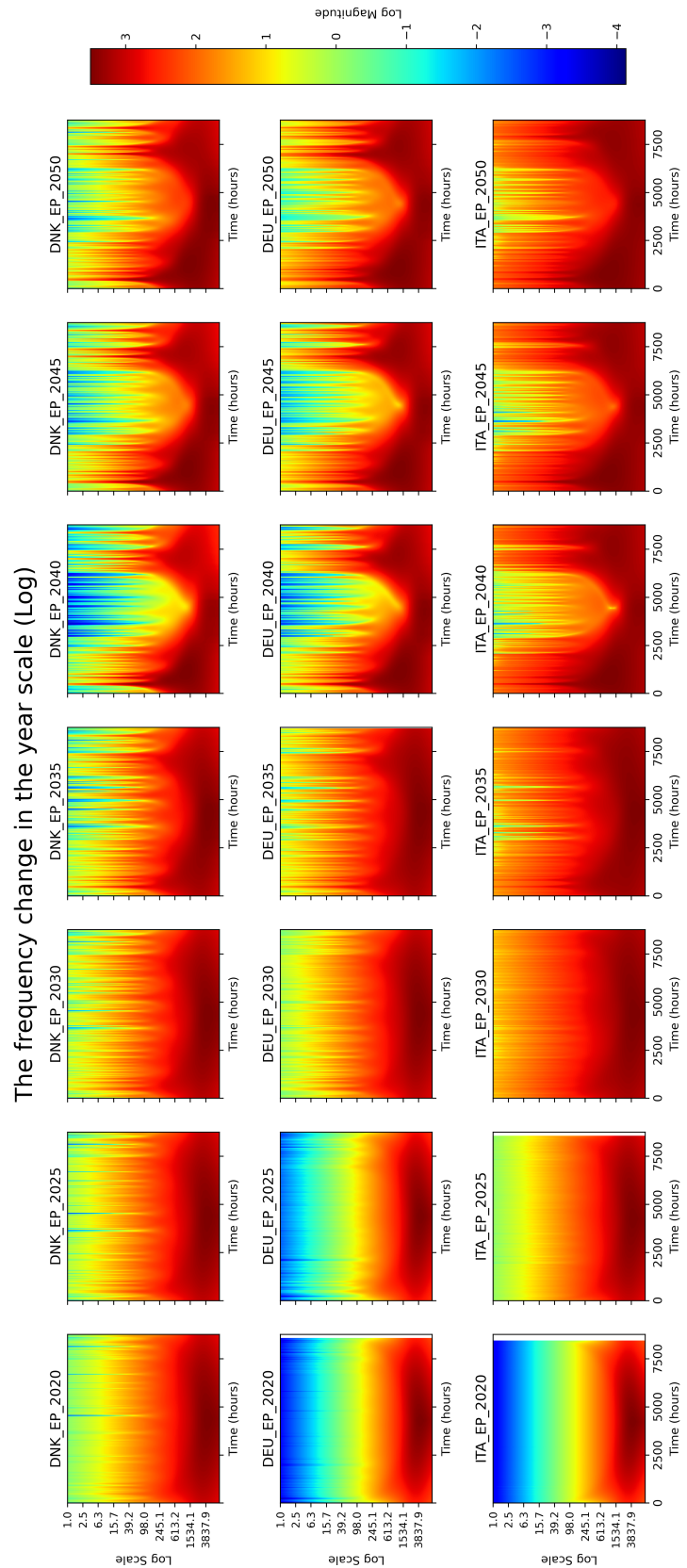


Figure S12. Continuous Wavelet Transform (CWT) Analysis of Electricity Prices in Denmark, Germany, and Italy

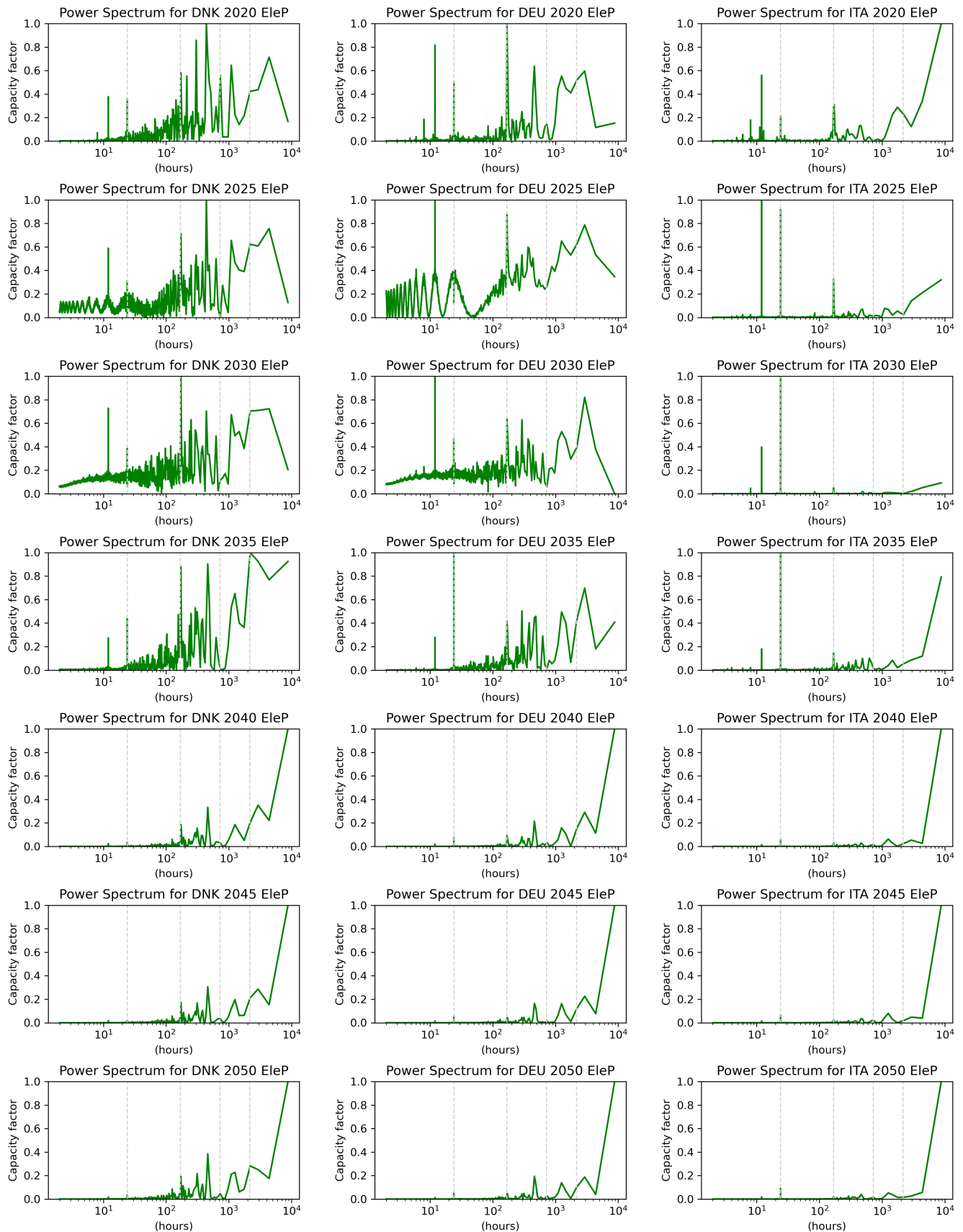


Figure S13. Fast Fourier Transform (FFT) Analysis of Electricity Prices in Denmark, Germany, and Italy

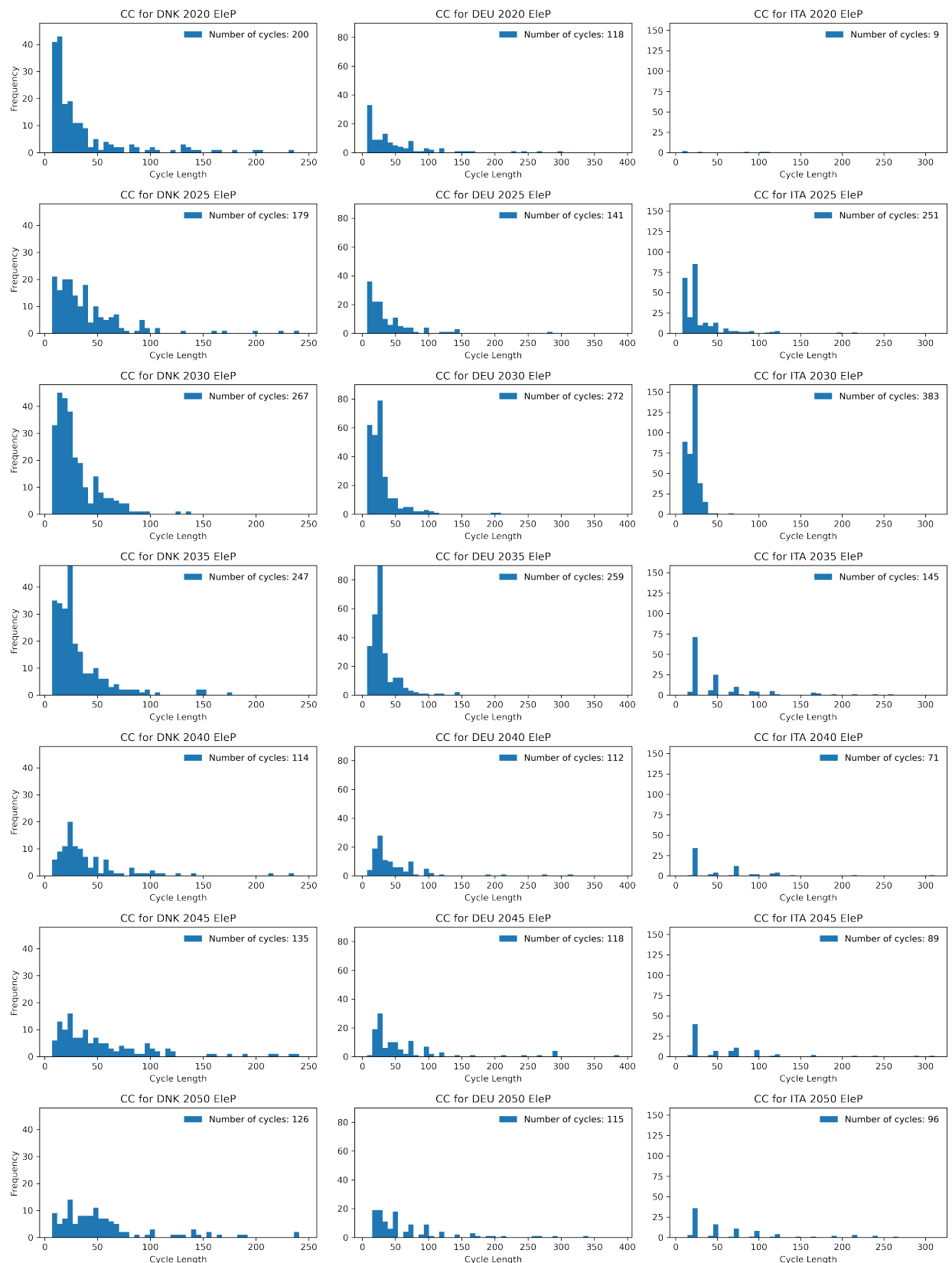


Figure S14. Cycle Capture (CC) Analysis of Electricity Prices in Denmark, Germany, and Italy

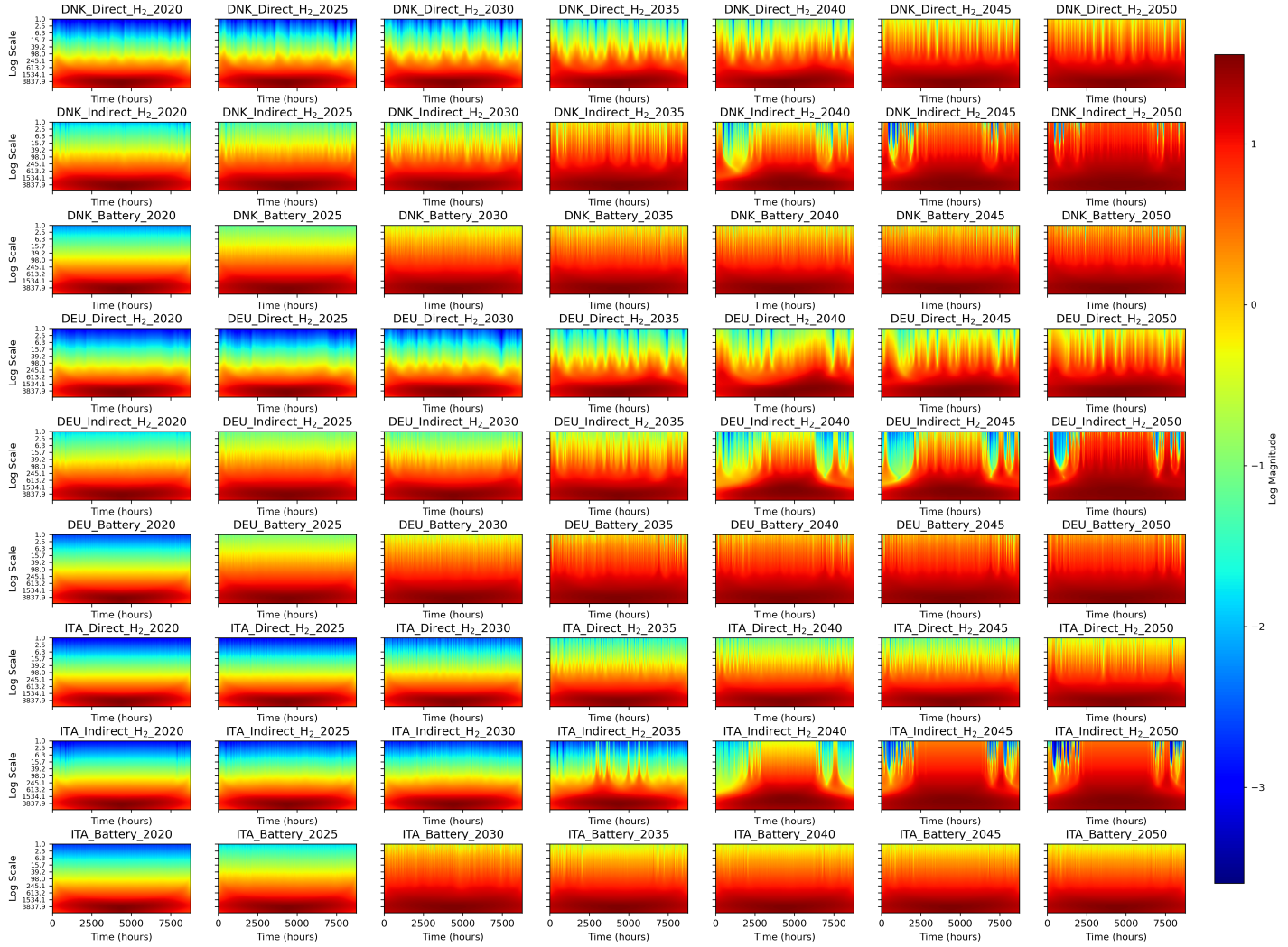


Figure S15. Continuous Wavelet Transform (CWT) Analysis of Storage Filling Level in Denmark, Germany, and Italy

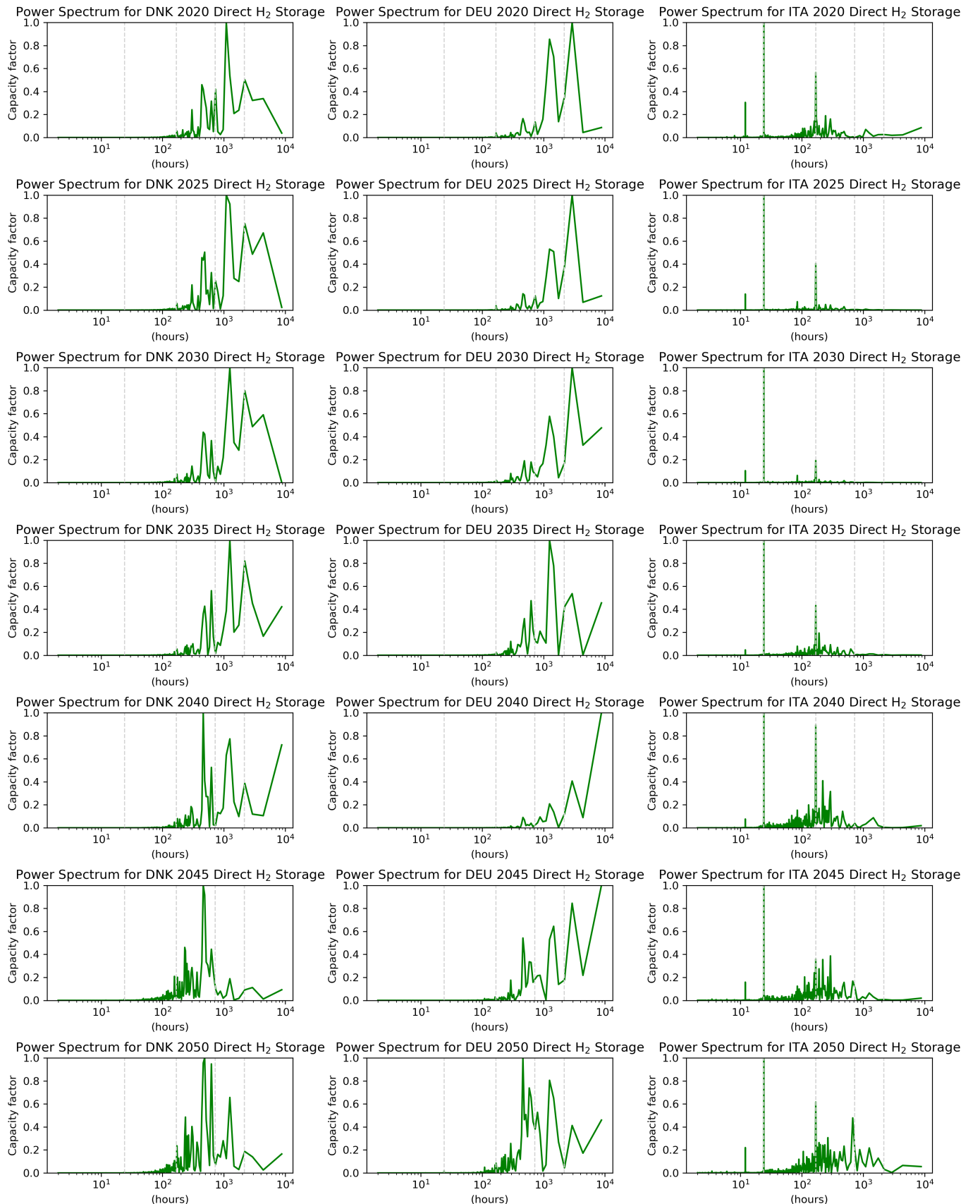


Figure S16. Fast Fourier Transform (FFT) Analysis of Direct Hydrogen Storage Filling Levels in Denmark, Germany, and Italy

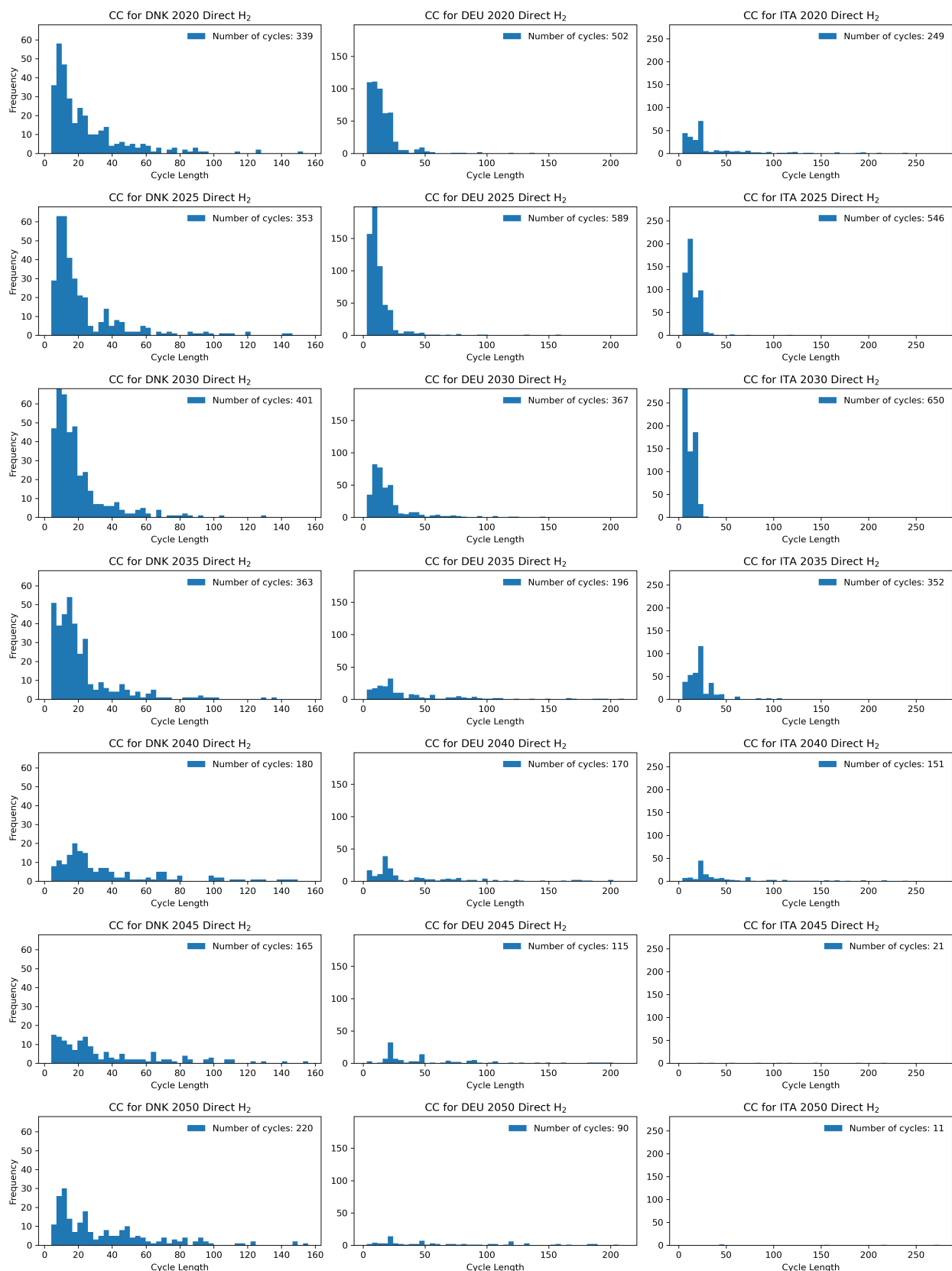


Figure S17. Cycle Capture (CC) Analysis of Direct Hydrogen Storage Filling Levels in Denmark, Germany, and Italy

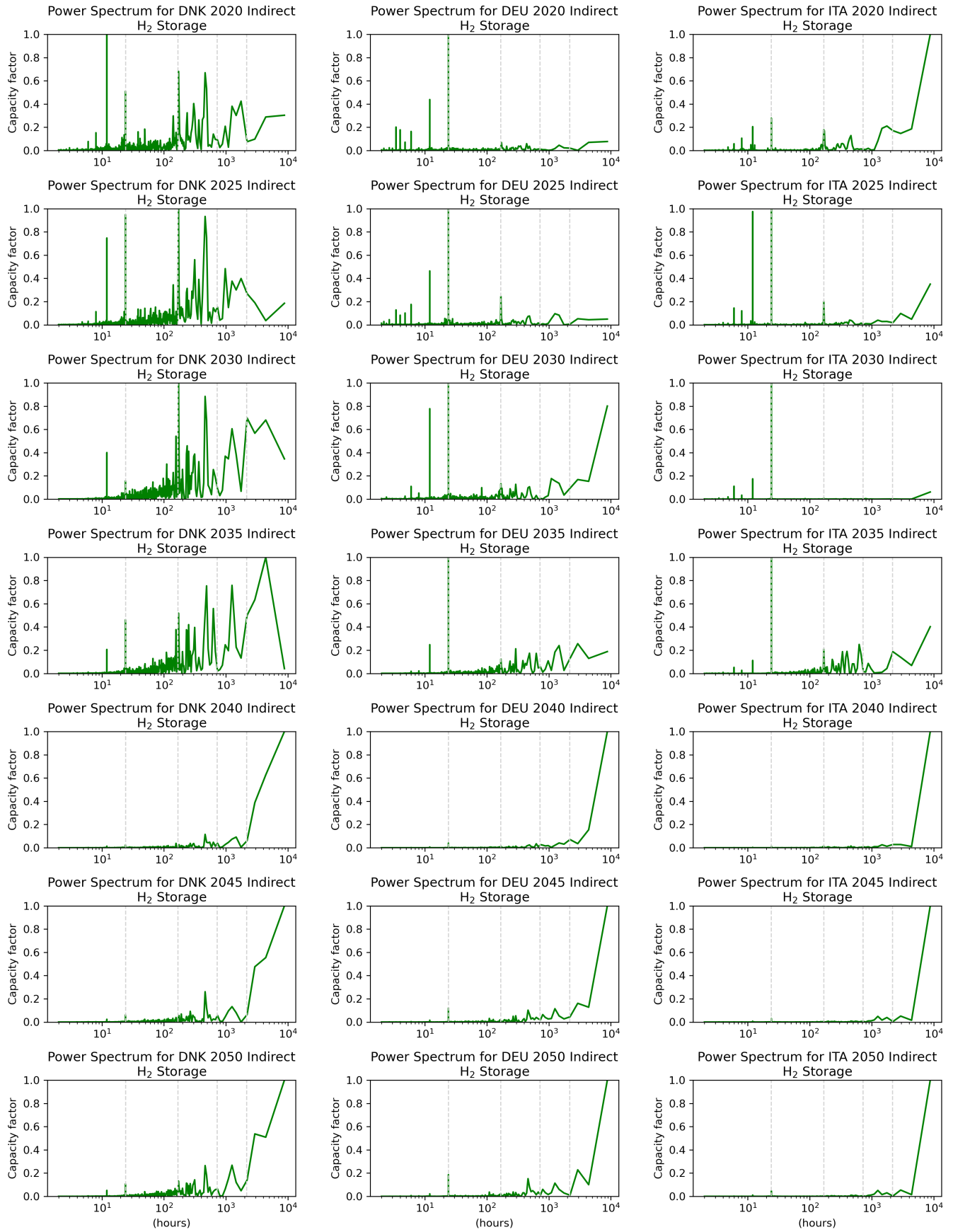


Figure S18. Fast Fourier Transform (FFT) Analysis of Indirect Hydrogen Storage Filling Levels in Denmark, Germany, and Italy

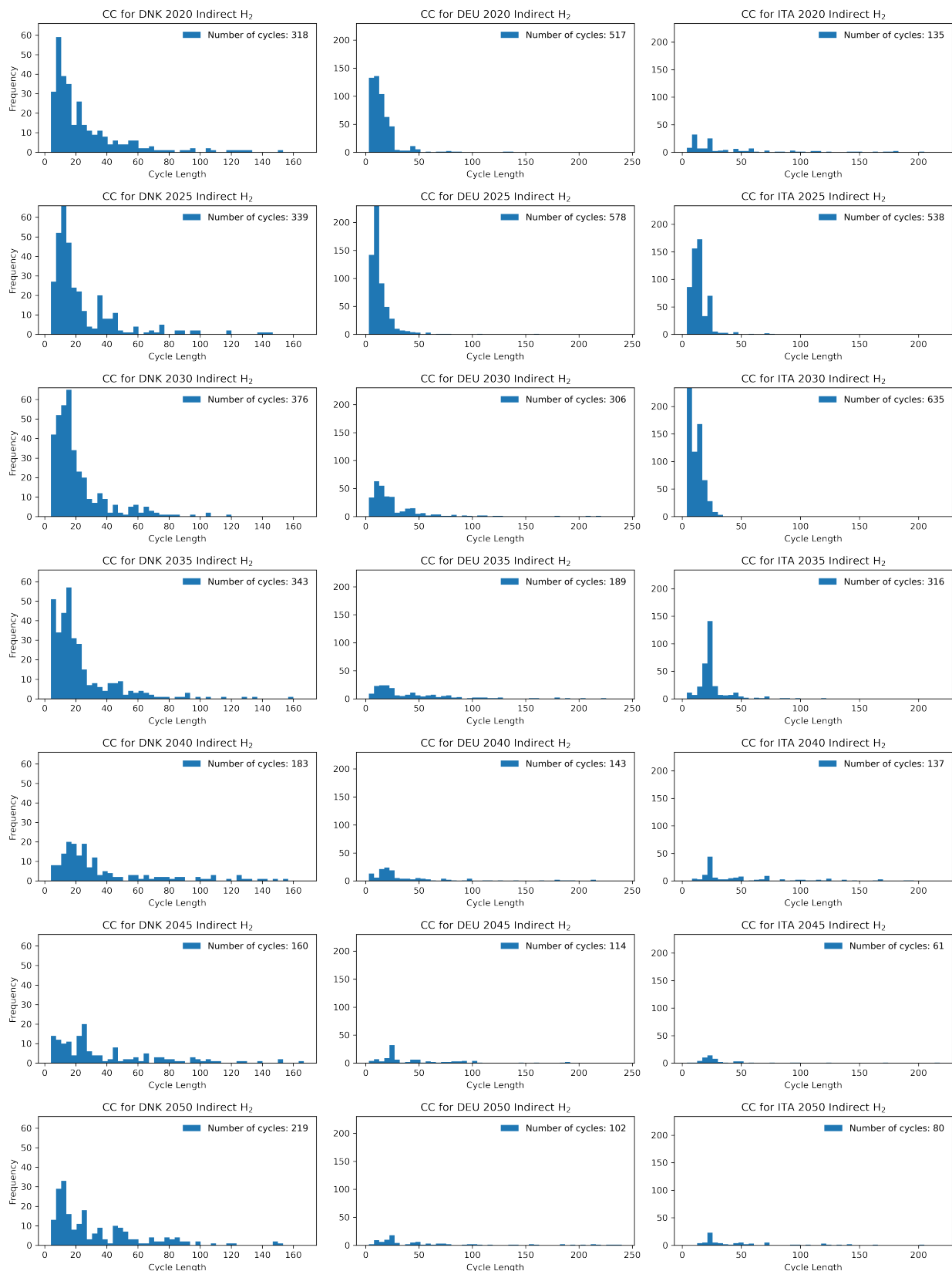


Figure S19. Cycle Capture (CC) Analysis of Indirect Hydrogen Storage Filling Levels in Denmark, Germany, and Italy

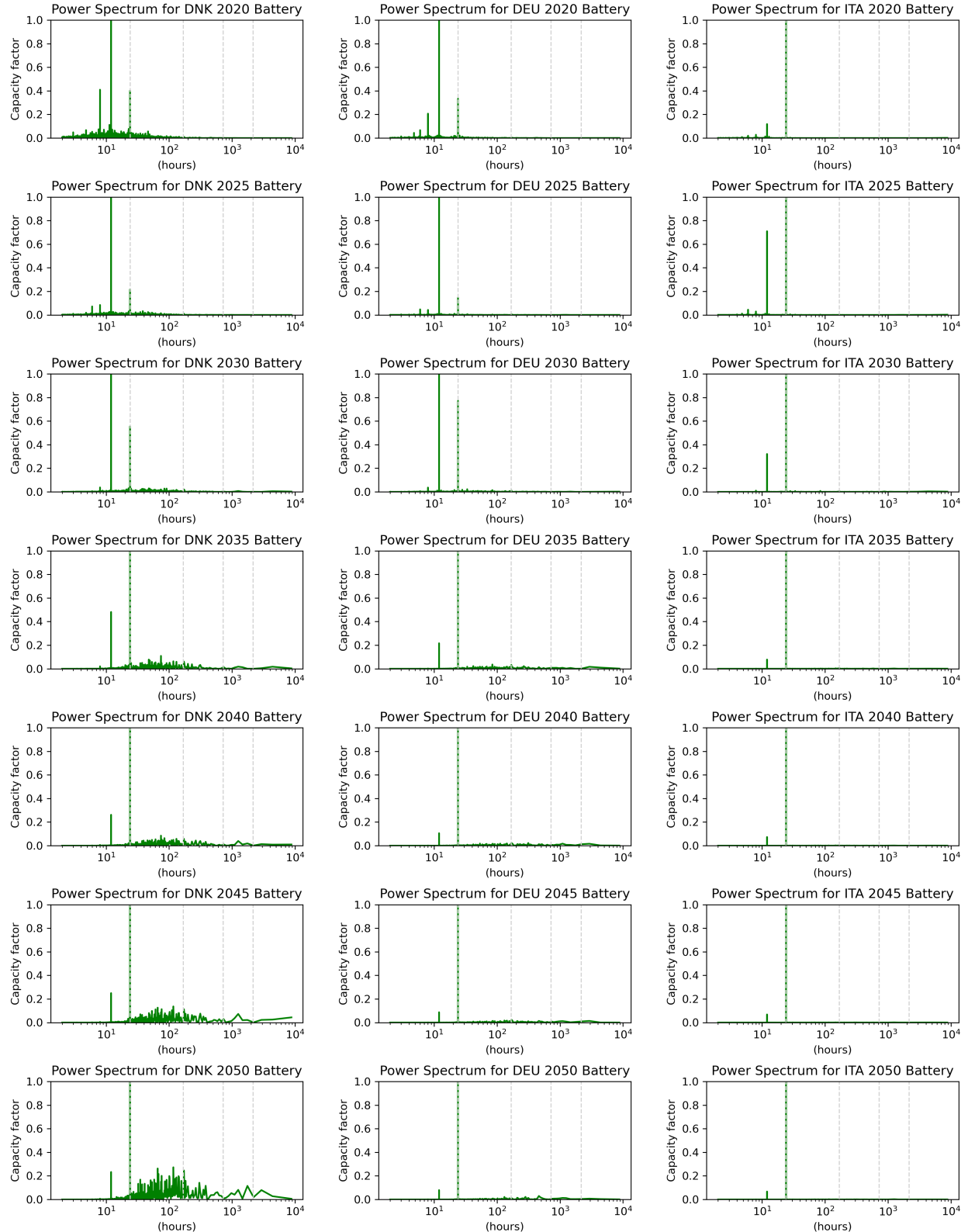


Figure S20. Fast Fourier Transform (FFT) Analysis of Battery Filling Levels in Denmark, Germany, and Italy

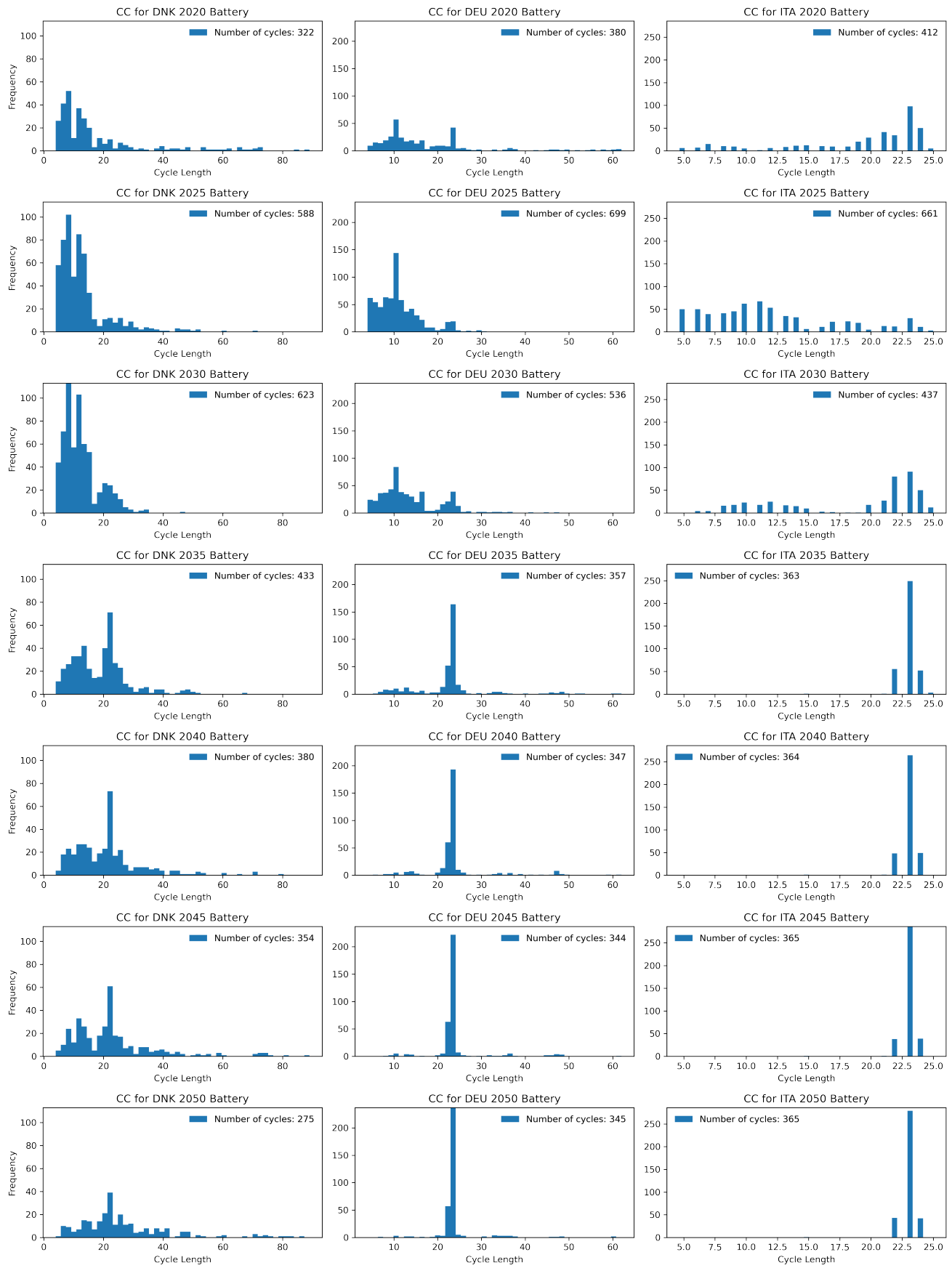


Figure S21. Cycle Capture (CC) Analysis of Battery Filling Levels in Denmark, Germany, and Italy

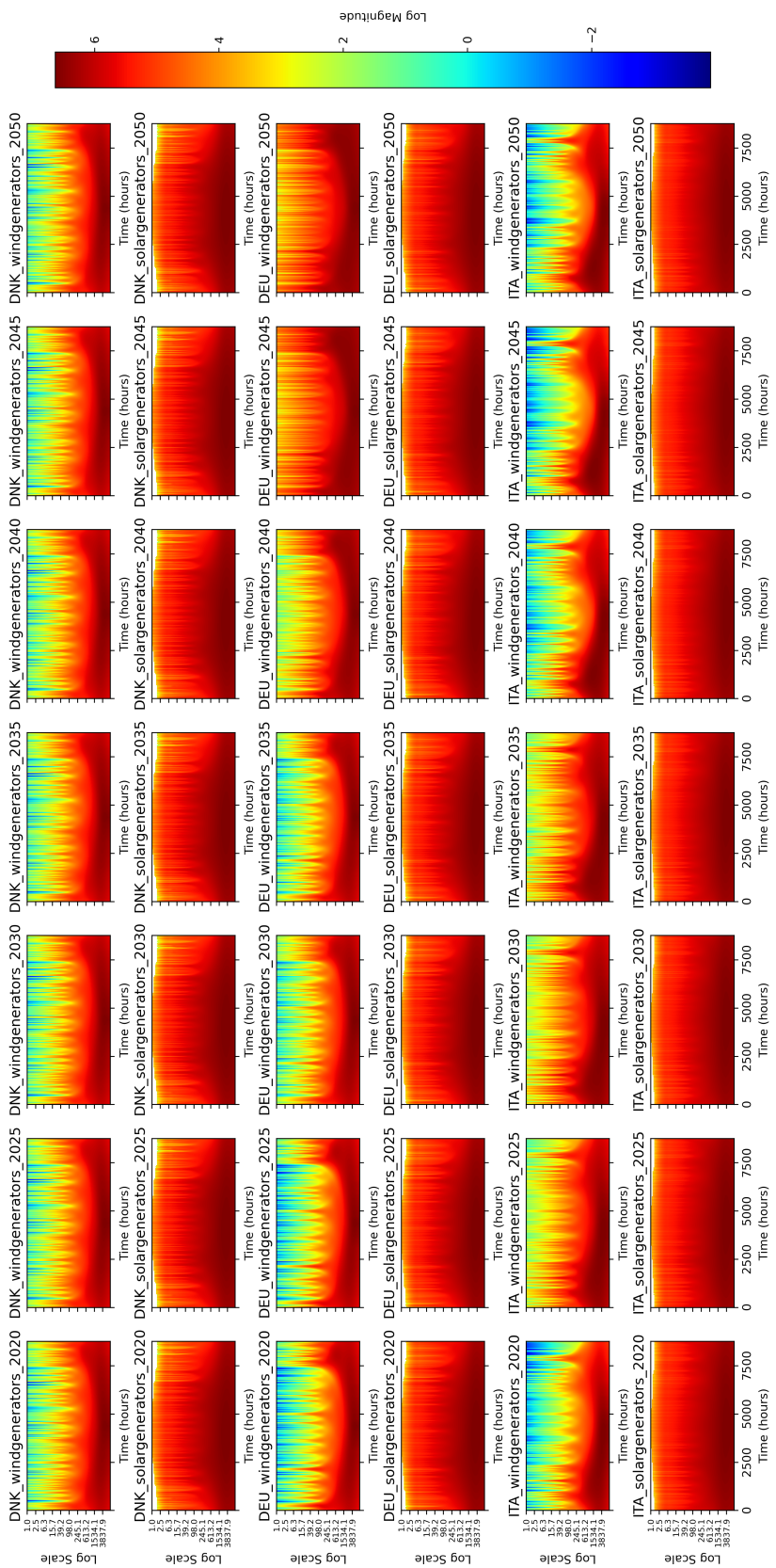


Figure S22. Continuous Wavelet Transform (CWT) Analysis of Renewable Energy Generation in Denmark, Germany, and Italy

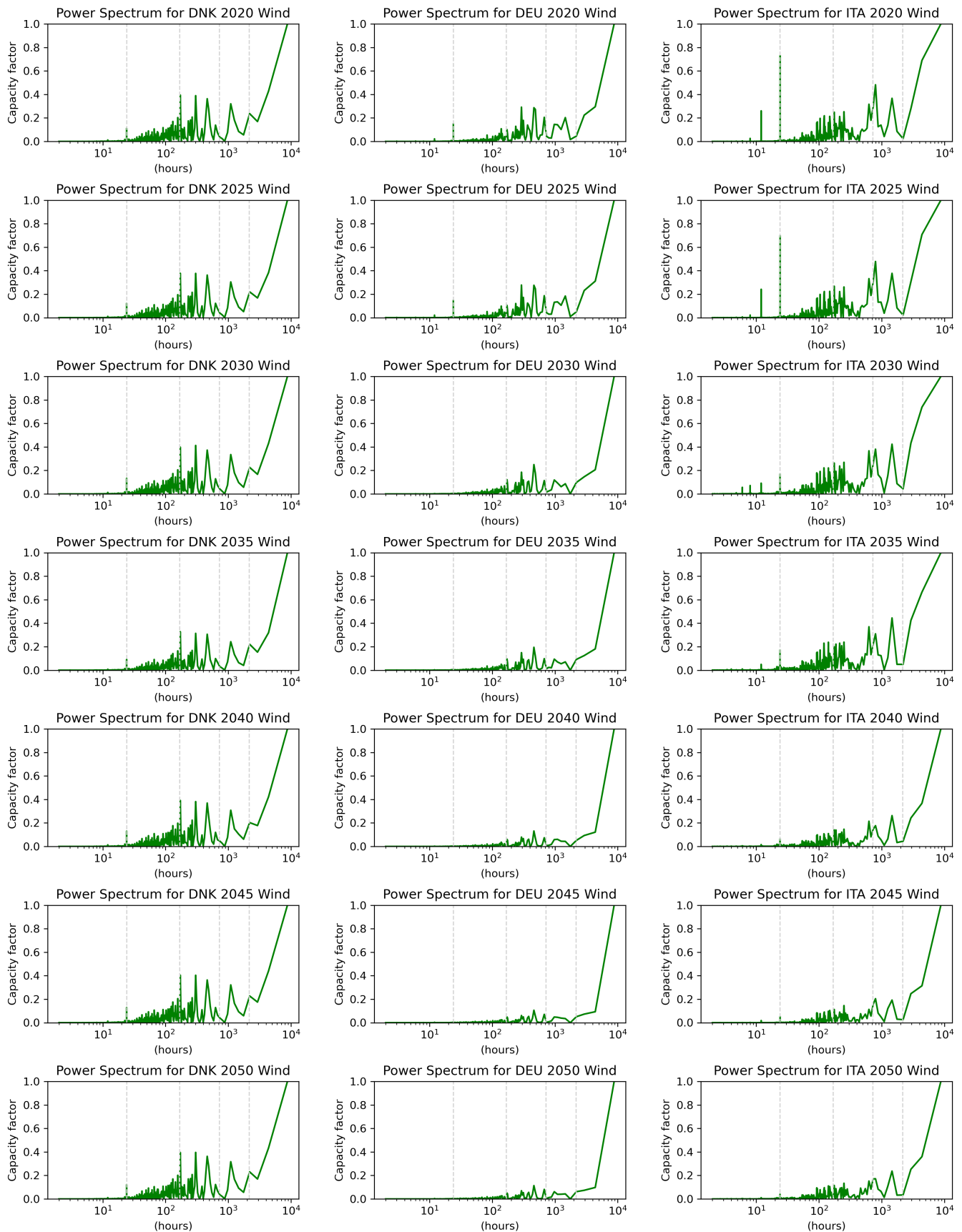


Figure S23. Fast Fourier Transform (FFT) Analysis of Wind Generations in Denmark, Germany, and Italy

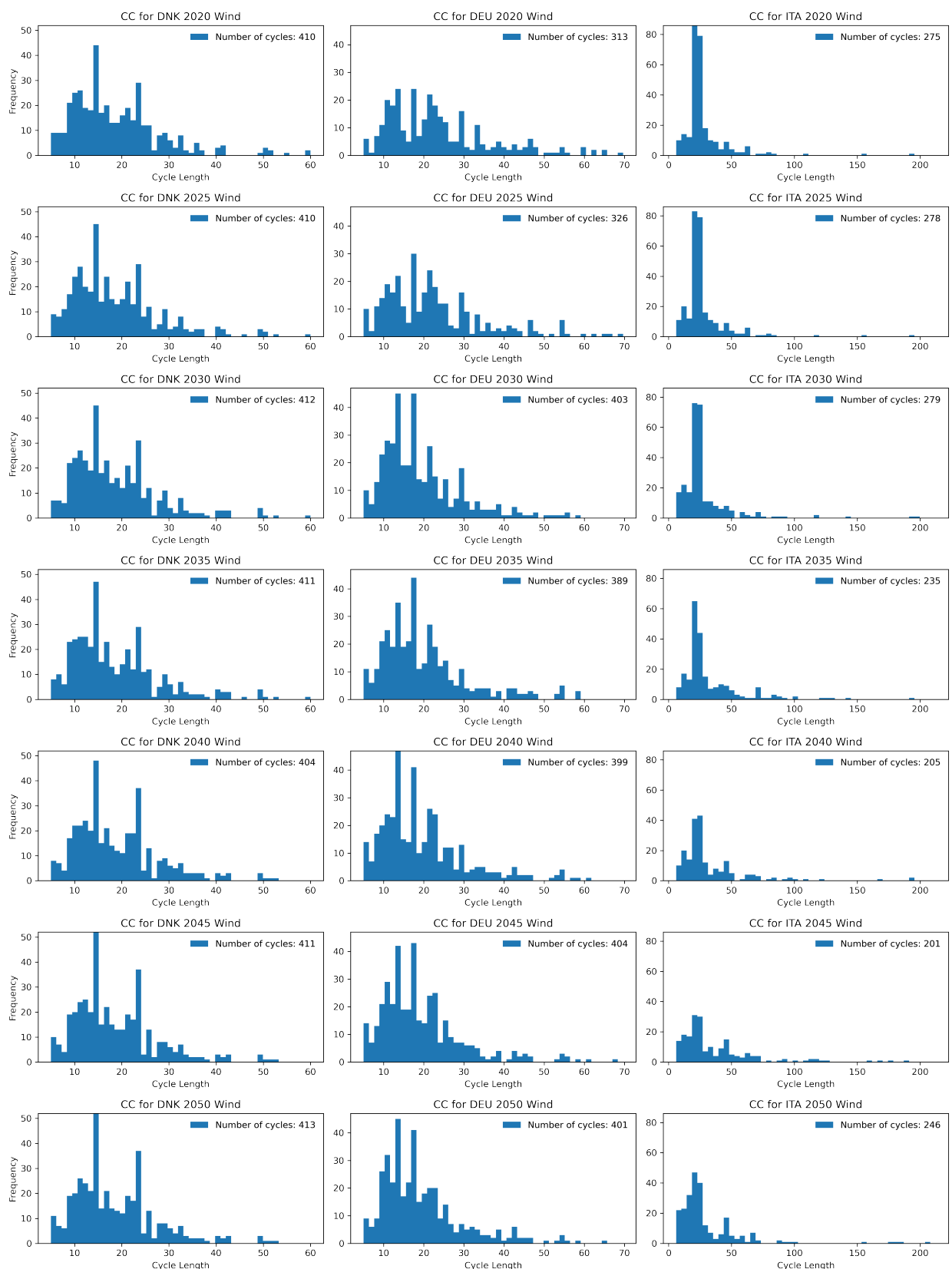


Figure S24. Cycle Capture (CC) Analysis of Wind Generations in Denmark, Germany, and Italy

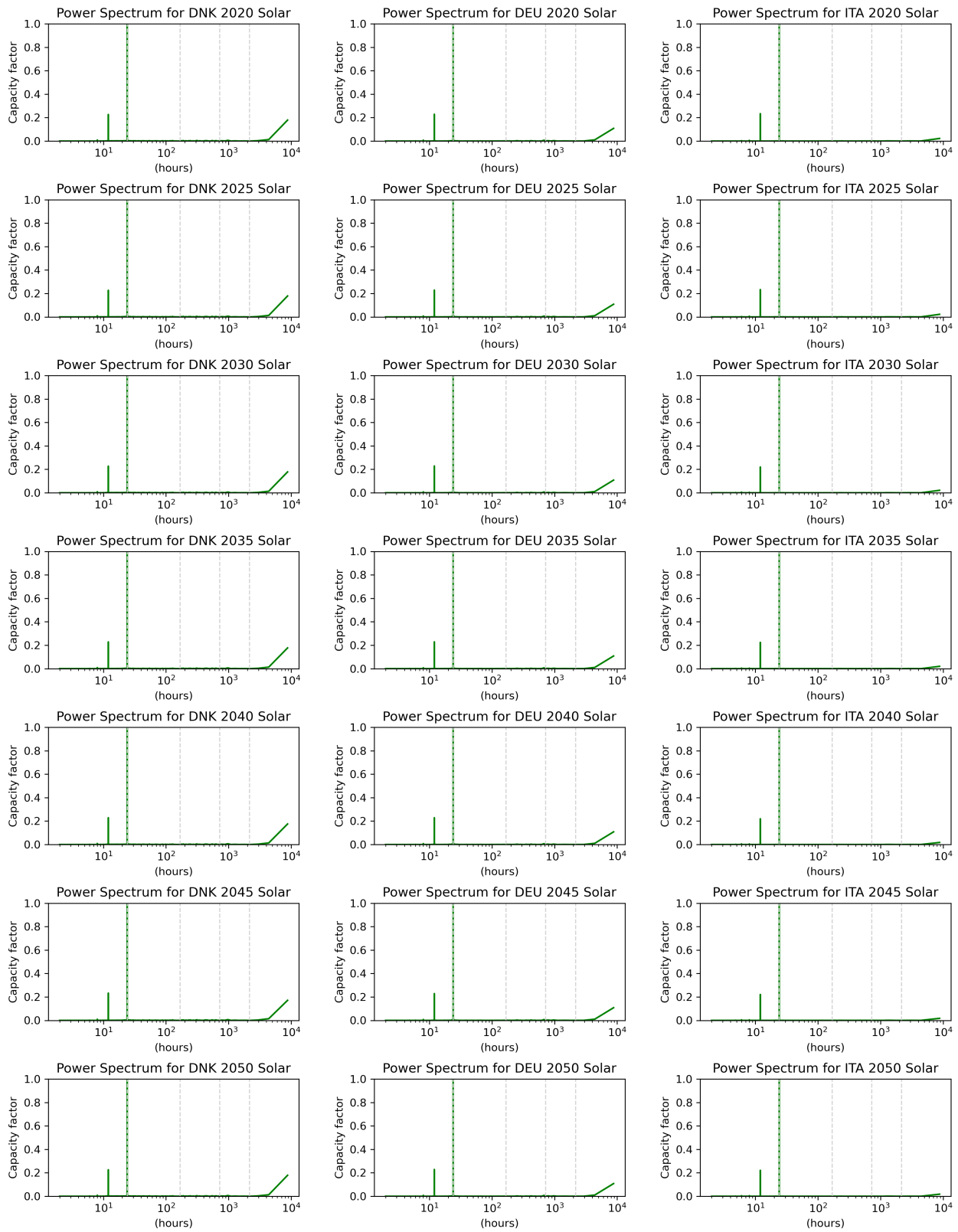


Figure S25. Fast Fourier Transform (FFT) Analysis of Solar Generations in Denmark, Germany, and Italy

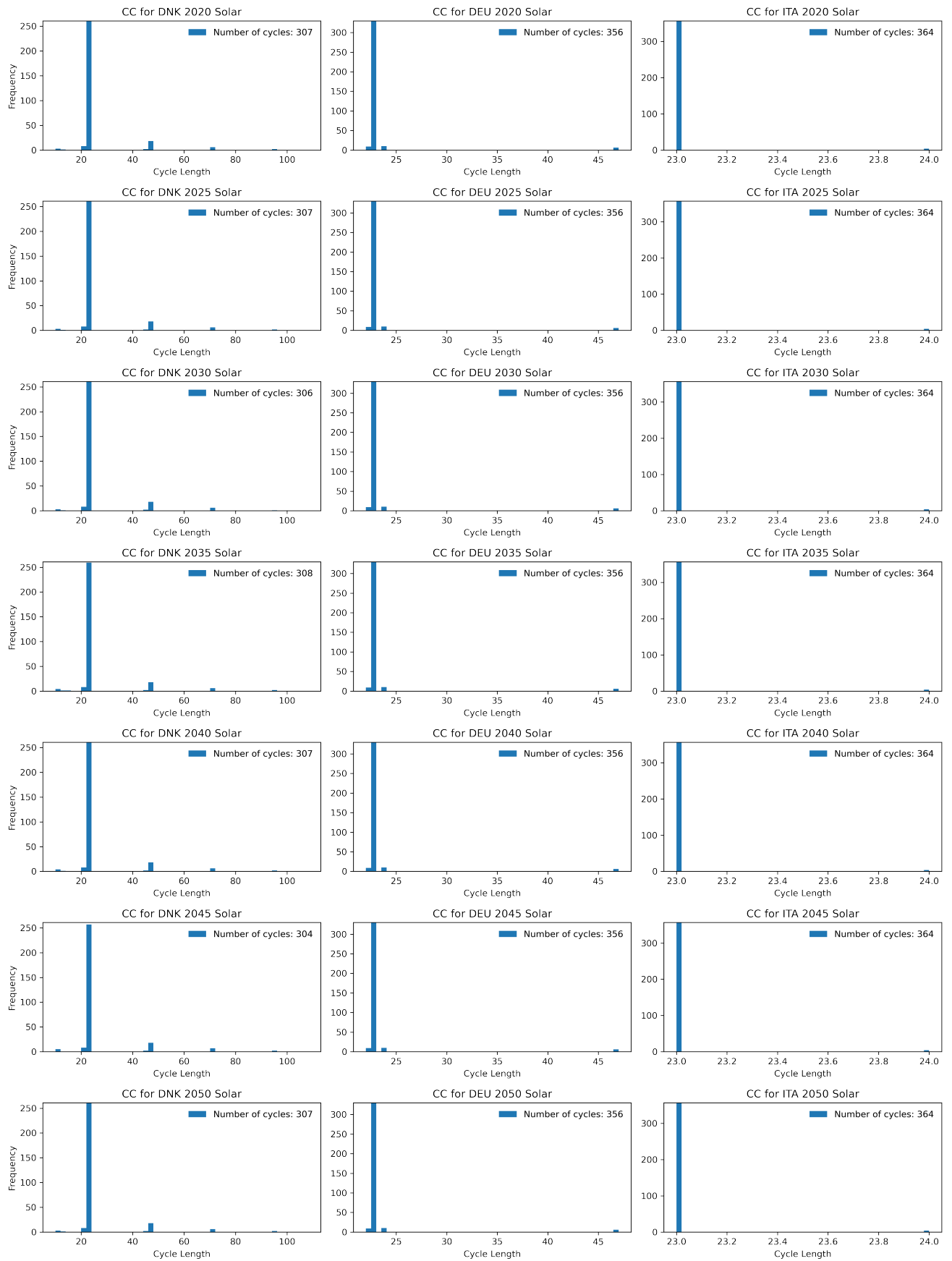


Figure S26. Cycle Capture (CC) Analysis of Solar Generations in Denmark, Germany, and Italy